DECOHERENCE AND ENTANGLEMENT IN SINGLE MOLECULE
MAGNETS

by

ÖZGÜR BOZAT

Submitted to the Graduate School of Engineering and Natural Sciences
in partial fulfillment of
the requirements for the degree of
Doctor of Philosophy

Sabanci University

August 2008

DECOHERENCE AND ENTANGLEMENT IN SINGLE MOLECULE MAGNETS

APPROVED BY

Assoc. Prof. Dr. Zafer Gedik

(Thesis Supervisor)

Assoc. Prof. Dr. Mehmet Ali Gülgün
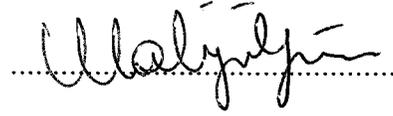
Assoc. Prof. Dr. İsmet İnönü Kaya

Prof. Dr. Cihan Saçlıoğlu
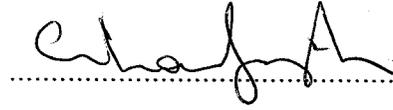
Assoc. Prof. Dr. Özgür Esat Müstecaplıoğlu

DATE OF APPROVAL: ...07./.08./.2008......

DECOHERENCE AND ENTANGLEMENT IN SINGLE MOLECULE MAGNETS

Özgür Bozat

Materials Science and Engineering, Doctor of Philosophy Thesis, 2008

Thesis Supervisor: Assoc. Prof. Dr. Zafer Gedik

Keywords: decoherence, entanglement, quantum tunneling, single molecule magnet, spin bath, phonon.

Abstract

Single molecule magnets are novel mesoscopic materials exhibiting both classical and quantum properties. Revealing the decoherence and entanglement mechanisms in these systems is crucial for the applications in quantum information technologies. In this thesis, quantum tunneling of magnetization is studied in single molecule magnet dimer $[Mn_4]_2$. Motivated by the recent experiments demanding the modification of the current theories, phonon mediated spin bath decoherence model is proposed.

In the first part of the thesis, the magnetization of the $[Mn_4]_2$ dimer under external magnetic field is investigated. Alternative entangled spin states involved in quantum tunnelings are identified by means of the exact solution of the Schrödinger equation and the Landau-Zener-Stückelberg method.

Later, a decoherence model is introduced in which the interaction between the single molecule magnet (central spin) and spin bath is mediated by phonons in a coherent state or thermal distribution. It is observed that the decoherence factor decays in a Gaussian fashion and it becomes independent of the phonon frequencies at short times for coherent states and low temperature thermal distribution. In the former case, if the phonon energies are much larger than spin-phonon coupling or bath spins are fully polarized, decoherence time becomes independent of the initial phonon state. For the thermal state case, phonons play more important role in decoherence with increasing temperature. Possible effects of the temperature on spin bath contribution to decoherence is discussed. Then, the effect of entangled environment on decoherence is analyzed. Entanglement within environment is shown to reduce the decoherence of central spin. Also, the entanglement dynamics of the

central bipartite spin system is studied. Classification of the Bell states is examined for common spin bath, and separate spin baths.

Last part of the thesis is the analysis of dephasing in entangled qutrits (three level quantum systems) under the classical noise, and quantum decoherence. Density matrix formalism is shown to give equivalent results for both cases. For common and separate baths, robust and fragile Bell-like qutrit states were determined, and Horodecki's bound entangled state is shown to be more robust to decoherence in the latter case.

TEK MOLEKÜL MIKNATISLARDA EŞEVRESİZLİK VE DOLAŞIKLIK

Özgür Bozat

Malzeme Bilimi ve Mühendisliği, Doktora Tezi, 2008

Tez Danışmanı: Doç. Dr. Zafer Gedik

Anahtar Kelimeler: eşevresizlik, dolaşıklık, kuantum tünnellemesi, tek molekül mıknatıs, spin banyosu, fonon.

Özet

Tek molekül mıknatıslar kuantum ve klasik özellikler gösteren yeni mezoskopik malzemelerdir. Bu sistemlerdeki eşevresizlik ve dolaşıklık mekanizmalarını açıklayabilmek kuantum bilgi teknolojilerindeki uygulamalar için çok önemlidir. Bu tezde tek molekül dimeri $[Mn_4]_2$'deki mıknatıslanmanın kuantum tünnellemesi çalışıldı. Mevcut kuramların değiştirilmesini gerektiren son deneylerden hareketle fonon yardımlı spin banyosu eşevresizlik modeli önerildi.

Tezin ilk kısmında $[Mn_4]_2$ dimerinin mıknatıslanması dış manyetik alan altında incelendi. Schrödinger denkleminin tam çözümü ve Landau-Zener-Stückelberg kuramı uygulanarak kuantum tünnellemesinde bulunan alternatif dolaşık spin halleri belirlendi.

Ardından tek molekül mıknatıs (merkezi spin) ve spin banyosunun fononlar yardımıyla etkileştiği eşevresizlik modeli sunuldu. Fononlar eşevreli halde veya ısıl dağılımda varsayıldı. Kısa zamanlarda, eşevreli haller ve düşük sıcaklık ısıl dağılımları alındığında eşevresizlik çarpanının Gauss türünde ve fonon frekanslarından bağımsız azaldığı gözlendi. Eşevreli durumda, fonon enerjileri spin-fonon etkileşmesinden çok büyük olduğunda veya banyo spinleri tamamen kutuplaştığında, eşevresizlik zamanının başlangıç fonon hallerinden bağımsız olduğu tespit edildi. Isıl hallerde artan sıcaklıkla beraber fononların eşevresizlikteki etkisinin de daha önemli olduğu görüldü. Spin banyosunun eşevresizliğe katkısının sıcaklıkla değişimi tartışıldı. Sonrasında dolaşık çevrenin eşevresizliğe etkisi incelendi. Dolaşık çevrenin merkezi spinin eşevresizliğini azalttığı gözlendi. Ayrıca iki parçalı merkezi spin sisteminin eşevresizliği çalışıldı. Ortak ve ayrı spin banyolarında Bell hallerinin sınıflandırılması incelendi.

Tezin son kısmında dolaşık kutritlerde (üç seviyeli kuantum sistemleri) evre kaybı klasik gürültü ve kuantum eşevresizliği altında analiz edildi. Yoğunluk matrisi yönteminin iki durum için de denk sonuçlar verdiği gösterildi. Ortak ve ayrı spin banyolarında kırılgan ve dayanıklı Bell benzeri kutrit halleri belirlendi. Horodecki'-nin bağlı dolaşık durumlarının ortak banyoda eşevresizliğe daha dayanıklı olduğu gösterildi.

to my family...

Acknowledgements

I would like to express my sincere gratitude to my advisor, Zafer Gedik, for his support and encouragement during all these years. I really appreciate his continuous confidence in me as a scientist, even at those times when my research studies were not going well.

I would like to thank all the faculty members of Materials Science and Engineering Program and Physics Program for their great efforts to create warm and friendly academic environment in Sabanci University.

Also, I would like to acknowledge my colleagues and friends, Karahan Bulut, Ender Gelgeç, İbrahim İnanç, Engin Karabudak, Yener Kuru, Çınar Öncel, Güngör Özer, and all the graduate students in our faculty, who made my time more interesting and enjoyable. I want to express my heartfelt gratefulness to Emel Yeşil for making everything beautiful, cheerful and hopeful.

Finally, my deepest gratitude goes to my family. I have been extremely fortunate to be surrounded by these amazing people. Once again, it is my pleasure to dedicate this work to them.

Contents

List of Figures

List of Tables

CHAPTER 1

Introduction

At the beginning of the 20th century most physicists believed that they well understood all the underlying fundamental rules of the nature. There were left just small details to be researched. However, this all changed with the paradigm shift from classical mechanics to quantum mechanics. Although this new theory was completely counter-intuitive to our experiences in the macroscopic world, to date, there is no single experiment contradicting the predictions of quantum mechanics.

One of the most bizarre properties of the quantum mechanics is the superposition principle which is the main reason of its inherently probabilistic nature. Absence of the superpositions in the macroscopic domain has been a long standing problem. Understanding the transition from quantum to classical (and the measurement problem in this context) is still the fundamental issue concerning the foundations of quantum mechanics. Copenhagen interpretation of the quantum mechanics, which assumed a clear distinction between quantum and classical world, has never been satisfactory [1]. However, the decoherence program, introduced by Zurek at 1981, is considered to solve most of this puzzle [2, 3]. This new approach does not assume any modification to standard quantum theory. Its main theme is simply that "no quantum system can be considered to be isolated from environment". Idealized notion of isolated physical systems has always been the guiding principle since the foundations of modern science. Indeed it was the reasonable approximation for the early years of the quantum theory where the experiments are usually performed on the microscopic systems. At these scales, physical systems do not interact much with their environments, and this leads to the observation of quantum effects. However, with increasing size of the system, it is no more possible to consider them as

isolated. This openness of the physical systems results in the lost of their coherence between the superposed states, and their behaving like classical objects.

Quantum entanglement is another important phenomenon intrinsic to quantum theory. Entanglement between two systems lead to a strong correlations among them in such a way that it is no more possible to attribute any physical description to the individual systems before the measurement, even when they are spatially well separated and do not interact. This strange behavior has been long discussed since the famous paper written by Einstein, Podolsky, and Rosen (EPR) in 1935 [4]. EPR proposed a thought-experiment with two entangled particles to demonstrate the lack of completeness of quantum mechanics. Although they considered the quantum mechanics as a correct physical theory, they concluded that it is unsuccessful because it is not complete. There were attempts to eliminate these seemingly non-local correlations, which were referred by Einstein as "spooky action at a distance", by the introduction of the local hidden variables. However, in 1964, John Bell introduced an inequality that must always be satisfied by local hidden variable theory while it can be violated by quantum mechanics [5]. Later it has been shown experimentally many times the violation of these inequalities thus disproving the existence of local hidden variables [6, 7, 8, 9, 10].

Quantum mechanics has had a profound influence on the era of electronic revolution and the photonics. Now it is warming up for the information age. Quantum computing, quantum communication, and quantum cryptography are rapidly evolving areas connecting information science and quantum mechanics [11]. For example in quantum computing, information is not manipulated discretely, as a series of zeros and ones (bits), but as continuous superpositions of them (qubits) where the number of possibilities is exceedingly greater. Various quantum algorithms has been proposed so far. One of them is Shor's algorithm in which the factorization of integer number can be performed exponentially faster than the best classical factoring algorithms [12]. This can cause a serious threat to electronic privacy and security since widely used public-key cryptography schemes are based on the difficulty of factoring integers.

There are numerous candidates for the physical realization of quantum computers. Among them, especially solid state systems (quantum dots, SQUID's, NMR's

etc.) have attracted a great interest due to their scalability which is an indispensable criterion for realistic quantum information processing. However, the most important drawback of these systems is their relatively strong couplings to the environment. Manipulating the spin degree of freedom, instead of charge degree of freedom, in solid state systems is a very convenient strategy due to long spin coherence times [13]. Recently, new type of magnetic materials, called as single molecule magnets (SMM's), has been the subject of intense research [14]. Bottom-up approaches enable to synthesize SMM's with well defined spin quantum states. Some of these molecules have spin dephasing times orders of magnitudes longer than the operation time of quantum logic gates [15, 16]. Therefore, they are the promising future elements of the quantum information processing. Microscopic spin quantum tunneling events lead to the observation of the macroscopic quantum tunneling of the magnetization [17, 18]. Tunneling mechanisms provide the quantum superpositions that are required for the realization of qubits. Recently, SMM dimers have been synthesized with entangled states due to intermolecular exchange couplings [19, 20, 21]. Entangled states are very important sources that can greatly enhance the use of the quantum information protocols over the classical ones. Their presence is essential for the realization of logic gates in quantum computers.

At temperatures well below the intramolecular exchange interaction energies, magnetic properties of the SMM is determined primarily by its spin ground state. Depending on the dominant type of the intra-molecular exchange interactions, ferromagnetic or antiferromagnetic, molecule can have high or low spin ground state, respectively. While the qubits can be realized in both types from the lowest lying spin states, qudits, multi dimensional quantum information processing units, can be constructed only from the high spin molecules. Qudits have many advantages over qubits. It is known that local realism is violated more strongly with increasing system dimensions [22, 23]. Entangled qudits are more robust to noise [23, 24], and they enhance the security in quantum cryptography [25, 26, 27, 28, 29, 30, 31, 32]. Also, by increasing the efficiency of quantum gates, they are promising elements for scalable quantum computers [33].

Objective of this thesis is three fold: Firstly, we aim to understand the details of the quantum tunneling of magnetization in $[Mn_4]_2$ dimer. Superexchange cou-

plings between Mn_4 SMM's link two molecules and lead to entangled spin states of the dimer. Clear identification of the entangled spin states taking part in quantum tunneling events is very important for the proper manipulation of them in quantum information protocols. We observe the contributions of the tunneling spin states that were omitted in previous studies. By examining the magnetization of the dimer, we also show that the multi-level spin states of the dimer can be considered as a network of two-level resonance points. Secondly, we investigate the decoherence process in SMM's. Understanding the mechanisms of interaction with environment is crucial for the implementation of error correction techniques [34] and/or error avoiding strategies [35]. Recent experiments showed that at very low temperatures (~ 20 mK), where only fluctuations are due to quantum tunnelings of SMM's spins, phonons have still critical effects on the decoherence of SMM's spins. It is speculated that relaxation of the electronic spins of SMM's to environmental spins might be possible through the lattice phonons. Accordingly, we propose a new decoherence model where the interaction between SMM (modeled as two-level system) and environmental spins is mediated by phonons. We analyze this model in detail for various central system and environmental states, and also for different limits of parameters in Hamiltonian. Final and the third objective of this thesis is to investigate the dephasing in entangled qutrits. As explained in the previous paragraph, making use of the excited levels of SMM has numerous advantages. Hence, we study the loss of phase relations in entangled qutrits due to interaction with classical noise and quantum environment. It is shown that, at the level of density matrix formalism, both external effects have same results on the central system.

Outline of this thesis is as follows: From Chapter 2 to Chapter 5, we review the preliminary concepts underlying the core study of the thesis. Chapter 2 covers the basic formalism of the quantum states. After presenting the distinction between the classical and the quantum states, we explain briefly the superposition principle. Then, we review the density matrix formalism and its relation to composite systems. Chapter 3 discusses quantum entanglement. First we give the formal definition of entanglement. Then, we summarize the ways of detecting and quantifying the entanglement for bipartite pure and mixed states. In Chapter 4, we explain the decoherence program. We introduce the concept of decoherence in relation to

quantum measurements. Also, a simple decoherence model is explained in order to understand the details of the program. Chapter 5 surveys the magnetization tunneling in SMM's. Decoherence and entanglement of magnetic molecules is discussed. Special emphasis is given to $[Mn_4]_2$ dimer in which two SMM's are in an entangled state. In Chapter 6, we study the spin tunneling mechanism in $[Mn_4]_2$ both numerically and analytically. We resolve the spin states in which quantum tunnelings take place. In Chapter 7, we propose a new decoherence model inspired by the recent experiments on SMM's where the decoherence due to environmental nuclear spins are mediated by phonons. We also investigate this decoherence model separately both for an entangled central system, and an entangled environment. In Chapter 8, we study the dephasing of the entangled qutrits (three level system), under classical noise and quantum decoherence. We classify the entangled states according to their robustness under such external effects.

CHAPTER 2

Quantum States

2.1 Quantum versus Classical States

In classical physics there is a one-to-one correspondence between the mathematical description of the state of a physical system and its observable quantities. Any system can be described completely by these measured quantities such as position, momentum, etc. However, in quantum mechanics, a physical system is described by an abstract state which is a vector in Hilbert space. Connection to the physical world is obtained through introduction of observables represented as Hermitian operators in Hilbert space. A measurement done on a system leads to the collapse of its state into one of the eigenstates of the measured observable with probability given by Born rule. These eigenstates have certain eigenvalues corresponding to measured physical quantity. So, connection of the quantum state to objective physical reality is obtained indirectly through introduction of measurement process. Still, this connection is not complete since many observables are mutually incompatible with each other. Mathematically, this is represented as non-commutativity of observable operators. Therefore, a quantum state can be a simultaneous eigenstate of a few observables. Unlike classical case, this prevents cataloging of an arbitrary number of physical properties to the system.

The probabilistic nature of quantum states has been interpreted as incompleteness of quantum mechanics in describing physical systems. One of the scientists sharing this idea was Einstein who had a famous quote "God does not play dice with the universe". Randomness of the measurement results on identically prepared systems tried to be explained by some hidden variable theories. They consider that

although systems have same quantum states, each system have some hidden variables whose values determine the result of the experiment. So, complete description of the physical system would consist of both quantum state and hidden variables. This would solve the indeterministic nature of quantum mechanics. However, as explained shortly with Bell's inequalities in the previous chapter, according to our current knowledge, quantum state provides a complete description of the physical system.

2.2 Superposition Principle

The superposition principle is one of the most fundamental concepts in quantum mechanics. It states that any two quantum states, $|\psi_1\rangle$ and $|\psi_2\rangle$, can be linearly combined in the form $c_1|\psi_1\rangle + c_2|\psi_2\rangle$, with complex coefficients c_1 and c_2, to form a new quantum state. By induction, the principle can be applied to arbitrary number of states such that if the states $|\psi_n\rangle$ represent a set of physical systems , then the superposition $|\Psi\rangle = \sum_n c_n|\psi_n\rangle$ also become a possible physical state. This principle emerges form the linearity of the Hilbert space which is formed by state vectors. The superposition state represents the simultaneous presence of its components and does not correspond to a classical ensemble of its components. If the latter was the case, namely proper mixture, then the superposition state would be in only one of its components with a certain probability. However, this is not the case. In order to distinguish quantum superposition from classical statistical distribution of the component states, the simultaneous presence of the components is referred to as a coherent superposition. Stern-Gerlach experiment, carried out by O. Stern, and W. Gerlach in 1922, is a very important and instructive demonstration verifying the existence of quantum superpositions. Another significant example is the double slit experiment performed by Akira Tonomura and co-workers at Hitachi in 1989 [36]. They observed interference patterns by sending the electrons through the double slit one at a time.

2.3 Density Matrix

In many situations quantum systems cannot be described by pure quantum states. These cases arise when we have insufficient information about which pure state describes the system. Then, we expect that the system is in one of the pure states $|\psi_n\rangle$, with respective probabilities p_n. Such a classical ensemble of pure states is called mixed state and represented by density matrix, or density operator, given by

$$\rho = \sum_n p_n |\psi_n\rangle\langle\psi_n|, \tag{2.1}$$

which is positive semi-definite Hermitian matrix with trace one. Density matrix representation is the most general description of the quantum system. Pure state corresponds to the case where only one of the probabilities is equal to one while the rest of them is equal to zero. Considering a pure state $|\Psi\rangle = \sum_n c_n |\psi_n\rangle$, its density matrix ρ becomes

$$\rho = |\Psi\rangle\langle\Psi| = \sum_{m,n} c_n c_m^* |\psi_n\rangle\langle\psi_m|. \tag{2.2}$$

The off-diagonal terms with $m \neq n$ are referred to as interference terms since they represent the quantum coherence between the different components.

2.4 Composite Systems

Now we give the description of a composite quantum system made up of two or more distinct physical systems. If we have N subsystems s_i, $i = 1, \ldots, N$ with corresponding Hilbert spaces $\mathcal{H}_{s_i}$ of dimensions d_{s_i}, the Hilbert space of composite system $\mathcal{H}_S$ is the tensor (or direct product) product of the Hilbert spaces of subsystems, i.e.,

$$\mathcal{H}_S = \mathcal{H}_{s_1} \otimes \cdots \otimes \mathcal{H}_{s_N}, \tag{2.3}$$

having dimensions of $d_{s_1} \times \ldots \times d_{s_N}$. Denoting the basis states of each subsystem as $|j_i\rangle_{s_i}$ with $j_i = 1, \ldots, d_{s_i}$, new basis of the composite system becomes $|j_1\rangle_{s_i} \otimes \ldots \otimes |j_k\rangle_{s_N}$. If each subsystem is prepared in the states ρ_{s_i} the joint density matrix of the total system ρ_S is given as

$$\rho_S = \rho_{s_1} \otimes \cdots \otimes \rho_{s_N}. \tag{2.4}$$

This density matrix corresponds to a state where none of the subsystems is correlated to another. In this simple case it is straightforward to retrieve the density matrix of

any subsystem that is interested. However, when the subsystems are correlated with each other, either classically or quantum mechanically, it is not trivial to retrieve the density matrix of the desired subsystem. In this case the density matrix of the subsystem is obtained via introducing the partial trace operation. This matrix is called the reduced density matrix. For instance, reduced density matrix of the nth subsystem is given by

$$\rho_{s_n} = Tr_{s_1 \ldots s_{n-1}, s_{n+1}, \ldots s_N} \left(\rho_S \right), \tag{2.5}$$

where $Tr_{s_1 \ldots s_{n-1}, s_{n+1}, \ldots s_N}$ is the partial trace operation over the whole subsystems except s_n, defined by

$$Tr_{s_1 \ldots s_{n-1}, s_{n+1}, \ldots s_N} \left(|\phi_1\rangle \langle \phi_1'|_{s_1} \otimes \ldots \otimes |\phi_n\rangle \langle \phi_n'|_{s_n} \otimes \ldots \otimes |\phi_N\rangle \langle \phi_N'|_{s_N} \right) = |\phi_n\rangle \langle \phi_n'|_{s_n}$$

$$\times Tr \left(|\phi_1\rangle \langle \phi_1'|_{s_1} \otimes \ldots \otimes |\phi_{n-1}\rangle \langle \phi_{n-1}'|_{s_{n-1}} |\phi_{n+1}\rangle \langle \phi_{n+1}'|_{s_{n+1}} \otimes \ldots \otimes |\phi_N\rangle \langle \phi_N'|_{s_N} \right),$$

$$\tag{2.6}$$

where $|\phi_i\rangle \langle \phi_i'|_{s_i}$ is any projector in the Hilbert space of subsystem s_i. Although the reduced density matrix cannot be considered as a complete description of the subsystem, this formalism gives the correct measurement statistics for the measurements performed on subsystems. It allows to address the components of the composite system, while this is not possible with the state vector representation.

CHAPTER 3

Quantum Entanglement

Quantum entanglement is considered to be the most bizarre aspect of quantum theory. In Schrodinger's words "Entanglement is not one but rather the characteristic trait of quantum mechanics". Entanglement refers to the situation where a composite system cannot be seen simply as the summation of its constituents. Subsystems cannot be attributed to quantum states of their own. It is only possible to talk about the state of the composite system. Subsystems are correlated such a way that measurement performed locally on one subsystem leads to a state reduction (collapse) of the whole system even when there is no interaction between the subsystems. Entanglement is also the central process underlying the decoherence phenomenon. In order to understand the basics of entanglement, we consider the simplest case of entanglement, namely the bipartite system which is composed of two level systems.

Let us consider two spin-$\frac{1}{2}$ particles with basis $|0\rangle_{s_i}$ and $|1\rangle_{s_i}$, $i = 1, 2$, corresponding to spin pointing up and spin down, respectively. First, we consider the pure states of the composite system. There are two distinct kinds of states for pure states. First one is product state, or separable state, of the form

$$|\Psi\rangle = |0\rangle_{s_1} \otimes |1\rangle_{s_2}, \tag{3.1}$$

which is written as tensor product of the subsystem states. For this state, we have maximal knowledge about the state of each subsystem and the composite system. The measurement results on different components are uncorrelated since a measurement performed on a component does not affect the others. However, it is not always possible to write the pure state of the total system as tensor product

of the subsystem states. Theses states are called entangled states. For instance consider the following states which are called as Bell states

$$|\Psi_{\pm}\rangle = \frac{1}{\sqrt{2}}(|0\rangle_{s_1} \otimes |0\rangle_{s_2} \pm |1\rangle_{s_1} \otimes |1\rangle_{s_2}) \qquad (3.2)$$

$$|\Phi_{\pm}\rangle = \frac{1}{\sqrt{2}}(|0\rangle_{s_1} \otimes |1\rangle_{s_2} \pm |1\rangle_{s_1} \otimes |0\rangle_{s_2}). \qquad (3.3)$$

One of the most striking facts about these states is that it is not possible to attribute any physical state to any subsystem. Although we have complete knowledge about the composite system, we have insufficient information about the subsystems. Local measurements performed on subsystems lead to a collapse in the total system state.

For mixed states of bipartite system, a separable state is defined as a convex sum of the product states $\rho_{s_1} \otimes \rho_{s_2}$ such that

$$\rho = \sum_i p_i \rho_{s_1}^i \otimes \rho_{s_2}^i, \qquad (3.4)$$

where convexity implies $\sum_i p_i = 1$ with $p_i > 0$. Any state that cannot be written in this convex decomposition form is defined to be an entangled state [37].

Extension of the entanglement definition to a multi-particle systems composed of more than two subsystems is straightforward. For n particle pure states, any state that cannot be written in a tensor product form $|\psi\rangle_{s_1}|\varphi\rangle_{s_2} \ldots |\phi\rangle_{s_n}$, and for mixed states any state that cannot be decomposed into a convex form of product states $\sum_i p_i \rho_{s_1}^i \rho_{s_2}^i \ldots \rho_{s_n}^i$ is defined as an entangled state[1]. However, entanglement of identical particles is a complicated problem. Correct characterization of the entanglement must exclude the non-factorization due to (anti)symmetrization [38].

3.1 Separability Problem

Although the definition of entangled and separable state is clear, in general it is difficult to determine whether a given state is entangled or separable.

Any bipartite pure state can be expressed as a sum of bi-orthogonal terms such that

$$|\Psi\rangle = \sum_i^d \lambda_i |\varphi_i\rangle_{s_1}|\phi_i\rangle_{s_2}, \qquad (3.5)$$

---

[1]In the rest of the thesis, except certain cases, we will not explicitly write the tensor product symbol $\otimes$ for the purpose of shorter notation.

where Schmidt coefficients λ_i are non-negative real numbers satisfying $\sum_i \lambda_i^2 = 1$ [39]. Here the summation index runs up to the dimension of the smaller subsystem. Schmidt coefficients can be easily computed from the reduced density matrices since $\rho_{s_1} = \sum_i \lambda_i^2 |\varphi_i\rangle\langle\varphi_i|_{s_1}$ and $\rho_{s_2} = \sum_i \lambda_i^2 |\phi_i\rangle\langle\phi_i|_{s_2}$. The number of nonzero values λ_i is referred to as the Schmidt number (or Schmidt rank). The Schmidt number allows us to distinguish separable states from entangled states. The state having the Schmidt number greater than one is the entangled state. Also, the maximally entangled state corresponds to one with all $\lambda_i = 1/d$. For the mixed states separability is still an unsolved problem. However, there are several criteria based on positive maps that can detect the large class of entangled states. One of them is positive partial transpose (PPT) criterion where the presence of at least one negative eigenvalue of the partial transposed density matrix implies entanglement [40, 41]. While PPT criterion is necessary and sufficient condition for bipartite system with dimensions 2×2 and 2×3, for higher dimensions it is only necessary one, i.e., there are entangled states having PPT which are called as bound entangled states [42]. Existence of bound entangled states having negative partial transpose is still an open problem [43, 44, 45]. Bound entangled states are not distillable, i.e., it is not possible to obtain any Bell state from arbitrary large number of copies of a given bound entangled state using local operations and classical communication (LOCC). However, it is possible to use them in quantum teleportation, and quantum cryptography. [46, 47, 48]. There is another criterion called as realignment criterion [49, 50] which is able to detect bound entangled states. It is defined as

$$R(\rho) = \max\{0, \|\rho^R\| - 1\}, \tag{3.6}$$

where ρ^R is defined as operation of realignment, i.e.; $(\rho^R)_{ij,kl} = \rho_{ik,jl}$, and double braces represents the trace norm of the operator. For separable states $\|\rho^R\|$ is always smaller than one.

Previous criteria usually require the reconstruction of the whole density matrix which is a difficult experimental problem. Instead, it is also possible to detect some of the entangled states by measuring the few observables of the system. This approach is called as entanglement witnesses [51]. An entanglement witness is a Hermitian operator such that its expectation value is negative for some entangled states while positive for every separable state.

3.2 Quantification of Entanglement

Quantification of the entanglement is one of the problems in quantum information with no general solution (for review see [52, 53]). Formally, entanglement measure is a nonnegative real function of a state which does not increase under LOCC, and is zero for separable states. There are two approaches to quantify the entanglement, operational approaches, and abstract approaches: In the former case, the entanglement of the state is measured according to its performance on a task which is impossible without the entanglement. Entanglement of formation [54], distillable entanglement [55], entanglement cost [55], and entanglement of assistance [56] are some of the examples for operational measures. Abstractly defined measures are listed as Von Neumann entropy [57, 58], concurrence [59], negativity [60], logarithm of the negativity [52], squashed entanglement [61], Rényi entropy [62], and relative entropy of entanglement [63]. Generally, abstract measures are bounds for operational measures. For example logarithm of the negativity is an upper bound to teleportation capacity [60], and an asymptotic entanglement cost under the set of PPT operations [64]. Another example is relative entropy of entanglement which is an upper bound for distillable entanglement [65].

For a bipartite system composed of two-level systems, concurrence is an easily computable entanglement measure [59]. For pure states, this measure is given as

$$C(\Psi) = |\langle\Psi|\tilde{\Psi}\rangle|, \tag{3.7}$$

where $|\tilde{\Psi}\rangle = \sigma_y \otimes \sigma_y|\Psi^*\rangle$ is referred to as the spin-flipped state. Here, σ_y is the second Pauli matrix, and $|\Psi^*\rangle$ is the complex conjugate of $|\Psi\rangle$. Generalization to mixed state is obtained through convex roof construction: from the set of average concurrences, where each elements is obtained from different decomposition of the total density matrix ρ, minimum valued is chosen,

$$C(\rho) = \inf \sum_i p_i C(\Psi_i), \tag{3.8}$$

where $\rho = \sum_i |\Psi_i\rangle\langle\Psi_i|$. Then, the concurrence is simply given by

$$C(\rho) = \max\{0, \lambda_1 - \lambda_2 - \lambda_3 - \lambda_4\}, \tag{3.9}$$

where the λ_i are the square roots of the matrix $\rho\tilde{\rho}$, indexed in order of decreasing size. Here, $\tilde{\rho}$ is spin-flipped density matrix given by $\sigma_y \otimes \sigma_y \rho^* \sigma_y \otimes \sigma_y$, where ρ^* is

the complex conjugate of ρ. Also, the entanglement of the formation E_f can be expressed in terms of the concurrence as $E_f = h(C(\rho))$, where $h(x) = -x \log_2 x - (1-x) \log_2 (1-x)$ has the form of binary entropy function.

Another commonly used entanglement measure is the negativity [60]

$$N(\rho) = \max\{0, \frac{\|\rho^{T_{s_i}}\| - 1}{2}\}, \tag{3.10}$$

where $\|\rho^{T_{s_i}}\|$ represent the trace norm of the partial transposed density matrix with respect to any subsystem. For the mixed states of two qubits, the negativity is bounded by the concurrence $N(\rho) \leq C(\rho)$, where the equality holds for the pure states [66].

CHAPTER 4

Quantum Decoherence

So far we introduced the preliminary concepts underlying the mechanism of decoherence. Now we are ready to explore the details of decoherence phenomena which is the key element of quantum to classical transition (for review see [67, 68]). We explore this transition in scope of measurement processes which converts the quantum states and quantum correlations into classical definite outcomes. Decoherence is nothing but an irreversible process of a measurement like interactions between the system and environment. So, in this chapter we first explain the quantum measurements, and then we explain the emergence of classical properties through decoherence.

4.1 Dynamics of Quantum Measurements

The standard description of measurement was introduced by von Neumann in 1932 [57, 58]. In contrast to Copenhagen interpretation that had assumed the measurement apparatus must be classical, von Neumann treated both the system and the apparatus in entirely quantum mechanical terms.

Consider a system with Hilbert space $\mathcal{H}_s$ spanned by orthonormal states $|s_i\rangle$ which our detector with Hilbert space $\mathcal{H}_d$ spanned by orthonormal states $|d_i\rangle$ is built to discriminate. Assuming that detector start form initial ready state $|d_0\rangle$, measurement interaction between the system and the detector will be of the form

$$|s_i\rangle|d_0\rangle \rightarrow |s_i\rangle|d_i\rangle. \tag{4.1}$$

As a result of the measurement there is one to one correspondence between the state of the system and the state of the detector. While the interaction due to the

measurement changes the state of the detector, the state of the system remains same. This type of measurement is called ideal von Neumann quantum measurement. It is also referred to as *pre-measurement* corresponding to the unitary part of the whole measurement process. If the system starts from a superposition state, the linearity of the Schrödinger equation implies the following scheme

$$\left(\sum_i c_i|s_i\rangle\right)|d_0\rangle \rightarrow \sum_i c_i|s_i\rangle|d_i\rangle. \tag{4.2}$$

Resulting state corresponds to an entangled state of the system and detector. It still does not represent a certain measurement result. Rather it represents the superposition of all possible measurement results. Such a superposition involving a macroscopic measurement device (Schrödinger cat states) is not something observed in nature. This nonobservance of the interference terms in macroscopic regime is one of the problems of von Neumann's measurement scheme. Other problem with this treatment is the so called *basis ambiguity* or *preferred basis problem*. In general, final state of the measurement scheme in Eq. (4.2) can be written in different bases such that

$$\sum_i c_i|s_i\rangle|d_i\rangle = \sum_i c_i'|s_i'\rangle|d_i'\rangle. \tag{4.3}$$

Each decomposition of the final state corresponds to different measured quantity. So, paradoxically, it is not possible to talk about which particular observable of the system is measured during the measurement process. Also, this freedom of choosing basis implies that the detector can simultaneously measure the non-commuting observables of the system, in apparent contradiction with the Heisenberg uncertainty relation.

Essential problem in von Neumann's treatment of measurement was the ignorance of the openness of the macroscopic measurement device. This deficiency was realized by Zurek via the introduction the decoherence theory [2, 3]. He extended the von Neumann's measurement scheme by introducing the environment as a third element in addition to central system and detector. Therefore, for an environment coupled to a detector, the new measurement scheme will be the following,

$$\left(\sum_i c_i|s_i\rangle|d_i\rangle\right)|E_0\rangle \rightarrow \sum_i c_i|s_i\rangle|d_i\rangle|E_i\rangle. \tag{4.4}$$

Corresponding density matrix of the combined system-detector will be

$$\rho_{s,d} = \sum_{n,m} c_m^* c_n |s_n\rangle\langle s_m| \otimes |d_n\rangle\langle d_m| \langle E_m|E_n\rangle. \tag{4.5}$$

In general, different macroscopic environmental states will be orthogonal to each other in time, i.e., $\langle E_m|E_n\rangle \approx \delta_{mn}$, then off-diagonal terms giving rise to an interference disappear, and above density matrix takes the form

$$\rho_{s,d} = \sum_n |c_n|^2 |s_n\rangle\langle s_n| \otimes |d_n\rangle\langle d_n|, \tag{4.6}$$

which only preserves the classical correlations between system and the detector. Final density matrix corresponds to an ensemble of measurement results $|s_n\rangle|d_n\rangle$. As a result only the single states $|d_n\rangle$ remain pure during time evolution. These states emerge due to special form of the interaction Hamiltonian giving rise to evolution in Eq. (4.4). They are called *pointer basis* or *preferred basis*. So, the decoherence theory solves both issues related to measurement problem, namely, nonobservance of the macroscopic interferences and basis ambiguity.

4.2 Simple Decoherence Model

Now we give simple example of decoherence model first introduced by Zurek in 1982 [3]. Although this model is simple and easily solved, it is important in capturing the essentials of decoherence theory, and realistic enough to explain certain experiments [69, 70]. It consists of a central two-level system S interacting with an environment E composed of N other two-level systems. Such an environment is referred to as "spin bath". Numerous physical systems can be represented by quantum two-level system, i.e., spin-$\frac{1}{2}$ particle, energy levels of atom, polarization of photon, position of electron in double quantum dot, etc. For the current discussion, we consider the most straightforward one, namely spin-$\frac{1}{2}$ particles, as our physical systems for both central system and environment.

We identify the basis states of S by $|\Uparrow\rangle$ and $|\Downarrow\rangle$, while we denote the basis states of environment with $|\uparrow\rangle_k$ and $|\downarrow\rangle_k$, $k = 1, \ldots, N$. Total system is described in 2^{N+1} dimensional Hilbert space $\mathcal{H} = \mathcal{H}_c \otimes \mathcal{H}_{E_1} \otimes \cdots \otimes \mathcal{H}_{E_N}$, where $\mathcal{H}_c$, and $\mathcal{H}_{E_i}$ represent the Hilbert spaces of the central system and i^{th} environmental spin, respectively. We assume that evolution of the total system is dominated by an Ising-like interaction

Hamiltonian H_{int} between the central system and bath spins. Therefore, we neglect the intrinsic dynamics of them and consider that the self Hamiltonians of subsystems disappear, $H_c = 0$, $H_{E_i} = 0$. Thus, the Hamiltonian of the total system has the form

$$H = H_{int} = (|\Uparrow\rangle\langle\Uparrow| - |\Downarrow\rangle\langle\Downarrow|) \otimes \sum_{k=1}^{N} g_k (|\uparrow\rangle\langle\uparrow| - |\downarrow\rangle\langle\downarrow|)_k$$

$$= c_z \otimes \sum_{k=1}^{N} g_k s_{kz}. \tag{4.7}$$

Here c_z, and s_{kz} are z-components of pauli operators in the form of

$$\begin{pmatrix} 1 & 0 \\ 0 & -1 \end{pmatrix} \tag{4.8}$$

for central system and k^{th} bath spin, respectively. $|\Uparrow\rangle$ and $|\Downarrow\rangle$ ($|\uparrow\rangle$ and $|\downarrow\rangle$) are the eigenstates of c_z (s_{kz}). g_k is the coupling strength between central spin and k^{th} spin which is a constant scalar.

According to our model Hamiltonian, environment monitors the c_z observable of the central system. Therefore, the eigenstates of the c_z will be the dynamically selected preferred basis. While they will be robust to decoherence, any superposition of them will be affected by the environment. Also, note that c_z commutes with the total Hamiltonian. This means that there will not be any change in the population of the central system, i.e., there will not be any exchange of energy between central system and environment. This type of models are referred to as pure dephasing model where decoherence takes place without any dissipation.

Assume that initial state of the total system is in the product form

$$|\Psi(0)\rangle = (a_\Uparrow |\Uparrow\rangle + a_\Downarrow |\Downarrow\rangle) \bigotimes_{k=1}^{N} (\alpha_k |\uparrow\rangle_k + \beta_k |\downarrow\rangle_k), \tag{4.9}$$

where the normalization of the wavefunction is satisfied by $|a_\Uparrow|^2 + |a_\Downarrow|^2 = |\alpha_k|^2 + |\beta_k|^2 = 1$. Time evolution of the state is given by applying the propagator e^{-iHt} to the initial state

$$|\Psi(t)\rangle = e^{-iHt}|\Psi(0)\rangle = a_\Uparrow |\Uparrow\rangle |E_\Uparrow(t)\rangle + a_\Downarrow |\Downarrow\rangle |E_\Downarrow(t)\rangle, \tag{4.10}$$

where

$$|E_\Uparrow(t)\rangle = |E_\Downarrow(-t)\rangle = \bigotimes_{k=1}^{N} (\alpha_k e^{ig_k t}|\uparrow\rangle_k + \beta_k e^{-ig_k t}|\downarrow\rangle_k). \tag{4.11}$$

18

In time, environmental wavefunctions, $|E_\Uparrow(t)\rangle$ and $|E_\Downarrow(t)\rangle$, become orthogonal to each other. This leads to creation of entanglement between the central system and the environment. Reduced density matrix of the central system is given by

$$\rho_c(t) = Tr_E\rho(t) = Tr_E|\Psi(t)\rangle\langle\Psi(t)|$$
$$= |a_\Uparrow|^2|\Uparrow\rangle\langle\Uparrow| + a_\Uparrow a_\Downarrow^* r(t)|\Uparrow\rangle\langle\Downarrow| + a_\Uparrow^* a_\Downarrow r^*(t)|\Downarrow\rangle\langle\Uparrow| + |a_\Downarrow|^2|\Downarrow\rangle\langle\Downarrow|. \quad (4.12)$$

The coefficient $r(t)$ determines the magnitude of the off-diagonal interference terms an it is called as *decoherence factor*. It is value is given by the overlap of the environmental states corresponding to pointer states

$$r(t) = \langle E_\Uparrow|E_\Downarrow\rangle$$
$$= \prod_{k=1}^N(|\alpha_k|^2 e^{i2g_k t} + |\beta_k|^2 e^{-i2g_k t}). \quad (4.13)$$

For sufficiently large N and random distribution of the couplings g_k, $r(t)$ follow an Gaussian decay with time [71]

$$|r(t)| \approx e^{-8t^2 \sum |\alpha_k|^2|\beta_k|^2 g_k^2}. \quad (4.14)$$

Thus, $r(t)$ decays rapidly to zero, and leaves the $\rho_c(t)$ diagonal in a mixture of the pointer states. Note that the $r(t)$ in Eq. (4.13) is a sum of periodic functions. This means that the $r(t)$ itself is also periodic in time, and it will eventually return its initial value of one. This period is called as recurrence time τ_{rec}. This time takes a small value if the initial state and the distribution of the coupling parameters are highly ordered. However, this is not the case for realistic systems. Indeed, τ_{rec} is generally extremely long time and of the Poincaré type with $\tau_{rec} \propto N!$. For macroscopic system τ_{rec} can exceed the lifetime of the universe. Therefore, decoherence is an irreversible process.

4.3   Modeling the Environment

Although decoherence processes including the interaction with environment are complicated many body problems to study, it is generally possible to simplify them by mapping onto a few canonical models. Environment can be modeled as a collection of spin-$\frac{1}{2}$ particles when the localized modes (spatially confined wavefunctions), such

as nuclear spin, paramagnetic spins, and defects are important [72, 73, 74]. In the opposite situation where the delocalized modes (spatially spread out wavefunctions) are dominant, such as electrons, phonons, and photons, it is possible represent environment as a collection of harmonic oscillators [75, 76, 77]. While both environment models affect the central system severely, their internal dynamics are significantly modified only for the case of spin bath. Among delocalized models, spin-boson model has been studied extensively, where the central two level system is linearly coupled to the environment of non-interacting harmonic oscillators [78, 79]. At low temperatures localized modes are typically a convenient environmental model [80]. In spite of numerous theoretical works, including both analytical approaches and numerical simulations [81, 82, 83, 84, 85, 86, 87, 88, 89, 90, 91], spin bath decoherence is still a hot subject. This is due to the rich dynamics of spin models with different intra-bath couplings.

CHAPTER 5

Single Molecule Magnets

Magnetism is one of the important playgrounds to study the transition from macroscopic classical properties to microscopic quantum properties. Single molecule magnets (SMM's) are mesoscopic materials showing both classical and quantum properties (for review see [14]). While they have classical well defined magnetization direction, and exhibit hysteresis loops, they also show quantum tunneling of magnetization and quantum phase interference.

SMM is organic molecule with magnetic centers which are metal ions with unpaired electrons. These ions are strongly coupled to each other mostly via oxygen atoms that can give rise to net spin S. The molecule possess uniaxial magnetic anisotropy due to crystal field effects [92] which leads to an energetically favorable easy-axis that the spin is preferentially aligned parallel to it. This structure is coordinated by a shell of organic ligands protecting the magnetic core from environment. Therefore, at temperatures well below the intramolecular exchange interaction energies, it can be considered as well isolated single domain magnetic particle. These identical nanomagnets can be packed in three dimensional crystalline structure where all the molecular easy-axes are aligned almost in the same direction. Hence it is possible to make an macroscopic observations while revealing the microscopic dynamics inside the nanomagnets. Below their blocking temperatures T_B (at the order of 1 K), they show very slow relaxation of the magnetization. First observation of the hysteresis loop was at 1993 [93]. While the origin of the hysteresis loops in traditional magnets are long range interactions, this observation was due to only short range interactions at the molecular level. Hysteresis loops imply that they can also be considered as an alternative to classical magnets for information

storage. It is also possible to work on these nanomagnets in various geometries other than 3D. Recently, it has been shown that they can be deposited on a surface to form two dimensional arrays [94]. Also, single electron transistor based on a SMM has been realized experimentally [95, 96].

Although SMM's have similar features to classical magnets, they also have many distinct characteristics peculiar to quantum mechanics. Spin tunneling is one of them. It has been observed that there are regular steps at the hysteresis loops of the magnetization [17, 18]. These steps are attributed to resonant spin tunnelings which occurs when the energy levels of the spin states on the opposite sides of the anisotropy barrier become degenerate. Another observed quantum effect is so called Berry phase oscillations, alternating constructive and destructive interference of different tunneling paths [97]. While these features make things more complicated in terms of reliability of information storage, it also opens new paths to study the transition from quantum to classical physics, and possible implementations as quantum information units [98, 99, 100]. Indeed, SMM's have been proposed as potential candidates for implementation of the Grover's search algorithm [100].

In this thesis we will focus on the high spin magnetic molecules where the exchange interaction between the core magnetic ions are predominantly ferromagnetic. First we will review the basic properties of these magnetic molecules without considering the effect of environment. Our discussion will include special references to molecules $[Fe_8O_2(OH)_{12}(tacn)_6]Br_8$ (tacn:1,4,7-triazacyclononane) and $[Mn_{12}O_{12}$-$(CH_3COO)_{16}(H_2O)_4]\cdot 2CH_3COOH\cdot 4H_2O$, in short Fe_8, and Mn_{12}, which are the mostly studied SMM's. Later we will discuss the effect of environmental interactions on the dynamics of the SMM's, and compare the theoretical studies with the experimental results. We will see that current theoretical framework needs to be extended to explain the recent observations on SMM's.

At low temperatures, single magnetic molecules can be described by single spin although they are composed of many spins. For instance Mn_{12} molecule is composed of eight Mn^{3+} ions having spin 2, and four Mn^{4+} having spin 3/2. Corresponding dimension of the Hilbert space is equal to 10^8 which is a huge number even for today's fastest computers. But we know that at sufficiently low temperatures well below the intramolecular superexchange energies, magnetic ions typically freeze along certain
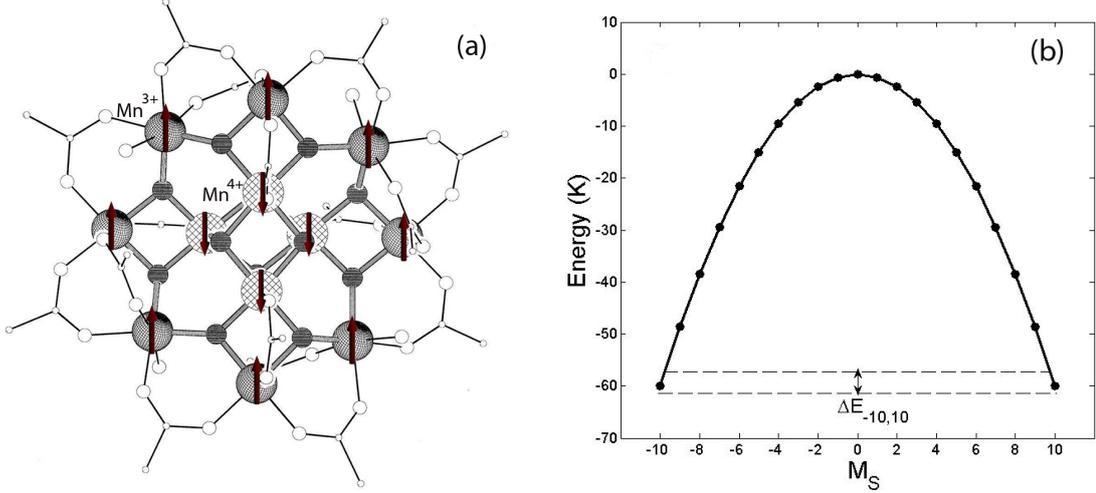
Figure 5.1: (a) Structure of Mn_{12} molecule. Small dark symbols are the bridging oxygen atoms while the open symbols are acetate ligands. (modified from reference [101]) (b) Energy spectrum of Mn_{12} molecule. Note that the tunneling splitting $\Delta E_{-10,10} \approx 10^{-10}$ K between the states $|M_S = -10\rangle$ and $|M_S = 10\rangle$ is not scaled in the figure for the purpose of visibility.

directions. Due to strong superexchange couplings between the ions, while eight Mn^{3+} spins becomes parallel to each other, the other four Mn^{4+} become antiparallel to them. This leads to a ground state having total spin S which is equal to $8 \times (2) - 4 \times (3/2) = 10$. So, it is possible to describe the molecule with effective single spin Hamiltonian. Then, the lowest energy levels of the molecule can be described approximately with the following Hamiltonian

$$H = -DS_z^2 - g\mu_B B S_z, \tag{5.1}$$

where D is positive valued uniaxial anisotropy parameter, g is Landè g-factor, and μ_B is the Bohr magneton. Uniaxial anisotropy parameter D is also called zero-field splitting since it removes the degeneracy of the S multiplet. Approximate values of D are 0.6 K and 0.3 K for Mn_{12} and Fe_8, respectively. B is the external magnetic field applied along the easy-axis. Since this Hamiltonian commutes with S_z operator, they have the same eigenstates which are $|M_S = -S\rangle, |M_S = -S+1\rangle, \ldots, |M_S = S-1\rangle, |M_S = S\rangle$. Corresponding eigenvalues of the Hamiltonian are

$$E_{M_S} = -DM_S^2 - g\mu_B B M_S. \tag{5.2}$$

For $B = 0$, the resulting energy spectrum has S number of degenerate levels corresponding to pairs having opposite signs of M_S values. These degenerate levels are

separated by an energy barrier due to uniaxial anisotropy barrier. Applying a magnetic field along the +z direction, while energy levels at the right side of the barrier corresponding to positive M_S values starts to decrease, energy levels at the left side of the barrier corresponding to negative M_S values starts to increase, leading to population increase at the RHS of the barrier. If the temperature is much lower than the energy barrier then the only populated energy level will be the state with $M_S = S$. In this way molecule will be totaly magnetized along the +z direction. When the magnetic field is removed, the system relaxes to its thermal equilibrium point. At high temperatures above T_B, the relaxation rate τ^{-1} of the system is given by Arrhenius law, $\tau^{-1} = \tau_0^{-1} \exp(-\Delta E / k_B T)$ where energy barrier ΔE has maximum value of DS^2 for integer S, and $D(S^2 - 1/4)$ for half-integer S. So, these molecules behave like classical superparamagnets.

What makes the SMM's so interesting is that the relaxation of the magnetization does not occur solely due to thermal processes. At low temperatures below T_B, these molecules were also relaxing due to purely quantum mechanical effect, namely quantum tunneling mechanism. It has been realized that there were regular steps at hysteresis loops in magnetization curves. These regular tunnelings were only possible if the seemingly degenerate energy levels are coupled to each other. Indeed, there are very small energy differences between these states, called "tunneling splitting". Lift of degeneracy is possible by introducing non-diagonal anisotropy terms to the the naive Hamiltonian in Eq. (5.1). This non-diagonal term that does not commute with S_z is

$$(S_+^4 + S_-^4) \tag{5.3}$$

for Mn_{12} due to tetragonal symmetry of the lattice, where $S_\pm = S_x \pm iS_y$, and

$$(S_x^2 - S_y^2) \tag{5.4}$$

for Fe_8 due to a hard-axis anisotropy caused by a rhombic distortion. However, terms imposed by the lattice symmetries are not sufficient to explain all the steps in the hysteresis loops. Second and fourth order transverse terms cannot give rise to the tunneling splittings between the spin states $|M_S\rangle$ and $|M_S' = -M_S + n\rangle$, where n is an odd number. Therefore, additional mechanisms must be incorporated to explain these steps. Origin of these tunneling transitions is considered to be due to

hyperfine interactions with magnetic nuclei, i.e. (^{1}H, ^{2}H, ^{13}C, ^{55}Mn), dynamic interactions between the nuclei, and the dipolar couplings between different nanomagnets at different lattice points. However, it is noted that tunneling splitting in nanomagnets are orders of magnitude smaller than the hyperfine and dipolar interactions. For example, in Mn$_{12}$, the tunneling splitting between $|M_S = -10\rangle$ and $|M_S = 10\rangle$ states is at the order of 10^{-10} K while the energy scale of the hyperfine and dipolar interactions are at the order of 10^{-1} K. According to these huge mismatches between energy scales, it is not expected to observe any tunneling. Nevertheless, explanation to this problem came from the Prokof'ev and Stamp (PS) [72, 73, 74]. They attributed the observation of the tunneling to the fluctuating dynamics of the nuclear spins. These nuclear dynamics continuously changes the energy levels at the opposite sides of the barrier and create tunneling window at certain resonance times. It results in the square-root law for the relaxation of the magnetization at temperatures below T_B. Assuming that the sample starts from fully magnetized states, $M(0) = M_{sat}$, short time relaxation is given as

$$M(t)/M_{sat} = 1 - \sqrt{t/\tau}. \tag{5.5}$$

The tunneling probabilities can be calculated by applying Landau-Zener-Stückelberg (LZS) theory [102, 103, 104]. The original work by Zener concentrated on the electronic states of a diatomic molecule, while Landau and Stückelberg considered a scattering process of two atoms. However, their solution of the time-dependent Schrödinger equation of a two-level system is applicable to many systems, and it is an important tool for studying tunneling transitions. According to LZS theory tunneling probability from state M_S to M_S' is given by

$$P_{M_S \to M_S'} = 1 - \exp(-\frac{\pi(\Delta E_{M_S,M_S'})^2}{2\hbar|M_S - M_S'|\mathrm{d}B/\mathrm{d}t}), \tag{5.6}$$

where $\Delta E_{M_S,M_S'}$ is the tunneling splitting between two states and $\mathrm{d}B/\mathrm{d}t$ is the sweeping rate of the time dependent applied field. This model is shown to be very useful for measuring the tunneling splittings [97].

5.1 Decoherence in SMM's

The spin tunnelings discussed so far are generally incoherent due to very small values of the tunneling splittings. In incoherent tunneling, when the spin tunnels across

the energy barrier it stays there and does not tunnel back. So, it is crucial to obtain higher tunneling splittings in order to observe coherent tunneling where magnetic moment of the molecule oscillates between energy barrier. This can be achieved by applying high transverse magnetic field to the nanomagnet. It has been argued that it is possible to obtain a coherence window by applying transverse magnetic field where both phonon and nuclear spin mediated decoherence is minimized [105]. Indeed, the oscillations of the tunnel probability as a function of the transverse field has been demonstrated in Mn_{12} [106]. This observation is attributed to the topological quantum phase interference of two tunnel paths of opposite windings.

Recent experiment has shown very promising results on the possibility to perform hundreds of manipulations on SMM, before it becomes decoherent by environment. It has been demonstrated that Cr_7M heterometallic wheels, with M=Ni and Mn, have very long dephasing time (T_2) than previously predicted by theoretical calculations [15]. At low temperatures, realizing the dipolar couplings to ^1H nuclei as the main mechanism of the decoherence, deuterated samples have shown decoherence time up to 3 μs. Another observation of the long decoherence time in SMM's came from Bertaina et al [16]. Their study on V_{15} molecule showed Rabi oscillations between two lowest spin levels. This is the first demonstration of Rabi oscillations in magnetic molecules indicating the existence of high degree of coherence. By spacing the vanadium molecules far apart in a solvent, they suppressed the dipolar interactions between the vanadium molecules which is the main source of the decoherence.

Although bosonic and fermionic modes are considered to be effective at different time scales, recent experiments on Mn_4, Mn_{12}, and Fe_8 molecules show that these two mechanisms cooperate together [107, 108, 109, 110]. Time dependent specific heat, and NMR experiments show that electron spins, and nuclear spins are in thermal equilibrium with lattice phonons down temperatures as low as 20 mK. However, at these temperatures, the only fluctuations are due to temperature independent quantum tunneling of the central spin. Hence, there should be a mechanism for exchanging energy between the electronic spins, nuclear spins, and phonons through the tunneling of the central spin. This observation is not consistent with PS theory. According to PS model, central spin of the molecule relaxes to the spin bath directly. They argue that relaxation to phonons is possible only at longer time scales. These

observations suggest the proper extension of the PS theory in which nuclear-spin-mediated quantum tunneling is combined with creation or annihilation of phonons. In these insulating magnetic materials, direct relaxation of the nuclear spins to the lattice phonons is extremely slow at such low temperatures. This might be possible through the electron spin-lattice phonon channel. Also, it has been proposed that the Waller mechanism, modulation of the dipolar fields by atomic vibrations, can play an important role [111]. These findings motivated us to propose a new model (in Chapter 7) for describing the decoherence of a SMM. In our decoherence model, interaction between SMM and bath spin is mediated by vibrational phonons and it is descried by three-body interaction Hamiltonian. Interaction strength between SMM and bath spin is modulated by the displacement operators of phonons.

It is possible to give examples from different physical system in which the contribution of the lattice phonons are crucial to the interactions between localized modes. Phonon assisted hyperfine interaction in quantum dots is one of them [112]. Deviations of the nucleus positions due to lattice vibrations modify the hyperfine coupling with electron spin. Another example can be given from optical lattices where coupling strengths between spins trapped deep inside a confining potential change with lattice oscillations [113].

For systems having discrete energy levels at low enough temperatures it is always possible to consider them effectively acting as a two-level system. This truncation of the high energy levels to produce effective spin-$\frac{1}{2}$ Hamiltonian is possible if the temperature is much lower than the energy difference between second and third excited states. For SMM's, while the energy difference of the lowest lying two levels from the nearest excited state is at the order of 1 K, the temperatures at the experiments can go down to 10^{-3} K. Thus, SMM's are ideal systems that can be mapped onto a two level system. In turn, decoherence program in the SMM's is usually reduced to the study of open quantum dynamics of central spin-$\frac{1}{2}$ particle. Accordingly, in our phonon mediated spin bath decoherence model, central SMM is considered as spin-$\frac{1}{2}$ particle.

5.2 Entanglement in SMM's

Creation of controlled and switchable interaction between two qubits is one of the fundamental necessities for quantum computing. Indeed single qubit operations combined with controlled-not gates (which are two qubit operations) are enough to implement an arbitrary unitary operation on n qubits. Consequently, they are universal for quantum computation.

First controlled coupled single molecular magnets is dimerized [Mn$_4$O$_3$Cl$_4$(O$_2$-CEt)$_3$(py)$_3$]$_2$·2C$_6$H$_1$4, (EtCO$_2^-$ is propionate, py is pyridine), in short [Mn$_4$]$_2$,has been synthesized in 2002 [19]. A Mn$_4$ is a SMM containing three ferromagnetically coupled Mn$^{3+}(S = 2)$ ions and one Mn$^{4+}(S = 3/2)$ ion antiferromagnetically coupled to other three ions giving rise to well defined ground spin state of $S = 3 \times (2) - 1 \times (3/2) = 9/2$ [114, 115, 116]. This compound crystallizes in a hexagonal space group (R$\bar{3}$) in which the Mn$_4$ molecules are lying head-to-head on a crystallographic S6 symmetry axis. The resulting [Mn$_4$]$_2$ dimer is held together by six C−H···Cl hydrogen bonds, leading to an antiferromagnetic superexchange interaction between two Mn$_4$ units. The Cl···Cl approaches also contribute to this coupling. Since each dimer is well separated form neighboring dimers, interaction among them is negligible. Similar to all SMM's, [Mn$_4$]$_2$ displays superparamagnetic behavior at high temperatures, and steps in magnetic hysteresis loops below a blocking temperature ($\sim$ 1K). However, unlike isolated SMM's, it shows qualitatively different tunneling behavior. There is an absence of quantum tunneling at zero magnetic field, due to a static exchange bias field that each Mn$_4$ experiences because of its neighbor within the dimer. This bias shifts the positions of the steps, so that quantum tunneling occurs before the external magnetic field was reversed. It has been demonstrated via electron paramagnetic resonance and magnetization measurements using an array of micro-SQUIDs that quantum tunneling occurs between entangled states of the dimer [117, 118]. This result is very important from both the applications in quantum computing and fundamental points of view. In order to perform multi qubit operations intra-dimer exchange coupling must be coherently controlled. Current studies concern the optical switchabilty of this coupling [119]. Also, the response of the exchange coupling to the hydrostatic pressure has been analyzed via inelastic neutron scattering experiment [120]. It has been ob-
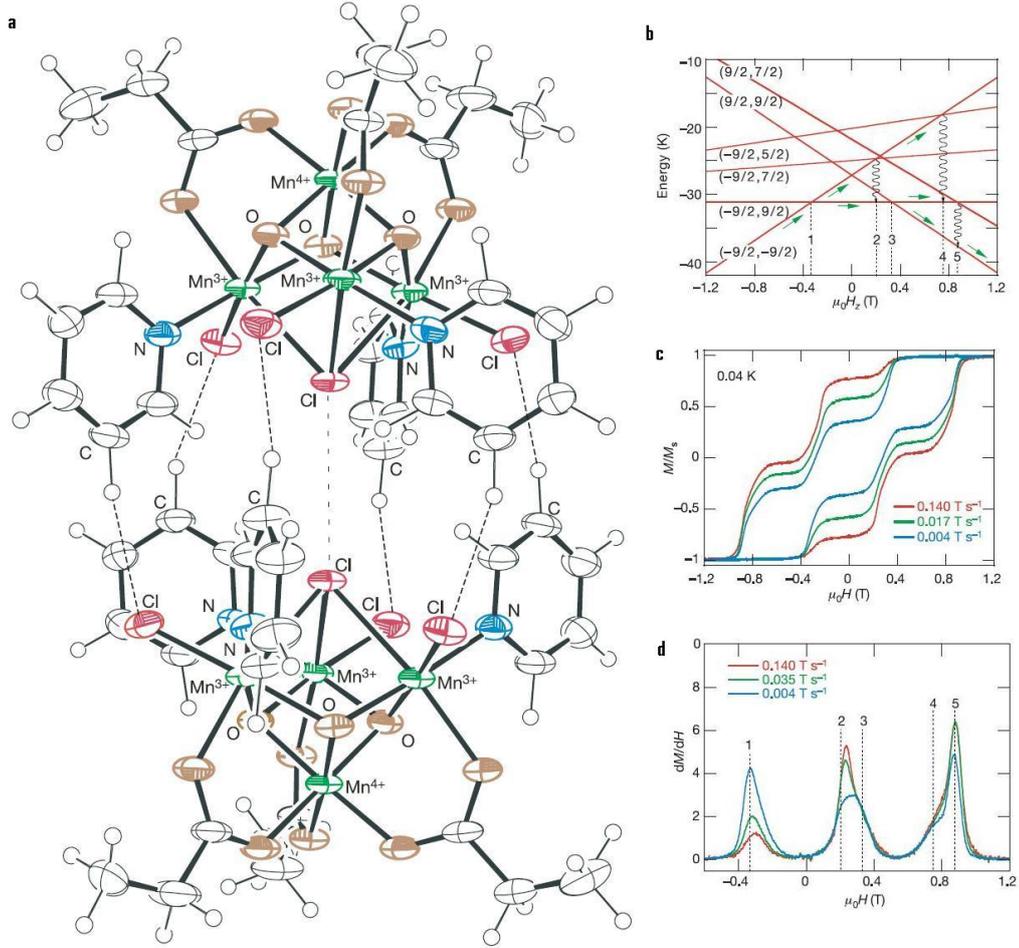
Figure 5.2: (a) Structure of the $[Mn_4]_2$ dimer. (b) Spin state energies of the dimer as a function of longitudinal magnetic field. (c)Magnetization versus longitudinal magnetic field at three different sweeping rates 0.140 T/s, 0.017 T/s, 0.004 T/s. (d) Derivatives of the magnetization curves for each sweeping rates (figures taken from reference [19]).

served that the exchange coupling strongly increase with pressure, up to 42% at 17 kbar.

Recently, another entangled dimer of SMM has been realized [20]. This new dimer is composed of two identical $[Fe_9O_4(OH)_4(O_2CPh)_{13}(heenH)_2]$ molecules, and called as $[Fe_9]_2$ in short. Interesting feature of this structure is that while 64% of the dimers in the crystal are exchange coupled (ON state)other 36% are not coupled (OFF state) to each other. The only difference between these ON and OFF states is the formation of single H-bond which leads to an antiferromagnetic exchange interaction. Finding a way to switch between these states is crucial problem to overcome.

Final example of the entangled SMM is Mn_{12} wheel [21]. It is claimed that each

half of the molecule behaves as a SMM and weak ferromagnetic exchange interaction between two halves leads to a dimeric structure. This leads to a quantum interference due to the quantum tunneling involving entangled states of the half-wheels. However, this new structure is the subject of a hot debate about the applicability of the dimer model in order to explain the certain observed resonance points [121, 122].

CHAPTER 6

Quantum Tunneling of Magnetization in $[\mathrm{Mn}_4]_2$ Dimer

In this chapter we will study the spin quantum tunneling process in $[\mathrm{Mn}_4]_2$ dimer by means of the exact solution of the Schrodinger equation and LZS theory. We will identify the spin states involved in tunneling process and reproduce the observed steps in the magnetization curve. Effect of the sweeping rate of the longitudinal external magnetic field on the heights and the positions of the steps will be discussed.

Single Mn_4 molecules has a well isolated ground state $S = 9/2$ separated at least 259 K from the lowest lying excited state $S = 8/2$. So, it can be modeled as single particle spin with $S = 9/2$ at temperatures well below the 259 K [114, 115]. This approximation reduces the dimension of the Hilbert space from $(2 \times (2) + 1)^3 \times (2 \times (3/2) + 1) = 500$ to $(2 \times (9/2) + 1) = 10$. The reduced Hilbert space of the Mn_4 is chosen to be spanned by the basis vectors $|M_S = -9/2\rangle, \ldots, |M_S = 0\rangle, \ldots, |M_S = 9/2\rangle$ which are the eigenstates of the z-component of the spin operator S_z. Corresponding Hamiltonian of the single Mn_4 molecule under the time dependent longitudinal external magnetic field $B_z(t)$ is given by

$$H_i(t) = -DS_{z,i}^2 - g\mu_B S_{z,i} B_z(t) + H_{trans,i}, \qquad (6.1)$$

where $i = 1, 2$ labels each Mn_4 of the dimer, $D = 0.72$ K is the uniaxial anisotropy constant, $g = 2$ is the Landè g-factor, $\mu_B = 0.67$ K/T is the Bohr magneton. Second term is the Zeeman term describing the interaction with $B_z(t)$, and $H_{trans,i}$ is the transverse term that does not commute with S_z, thereby causing the tunneling. We

assume the following form for this term

$$H_{trans,i} = E(S_{x,i}^2 - S_{y,i}^2) + g\mu_B S_{x,i} B_x. \tag{6.2}$$

First term is the second order plane anisotropy term with strength $E = 0.032$ K. Last transverse Zeeman term is introduced in order to account for the observed steps in the experiment. The origin of this term is due to the dipolar and the hyperfine interactions as we explained in the previous chapter. These environmental couplings act as a transverse magnetic field with strength $B_x = 0.035$ T [116].

Antiferromagnetic superexchange interaction between two Mn$_4$ molecule couples them and gives rise to a [Mn$_4$]$_2$ dimer with total Hamiltonian

$$H(t) = H_1(t) + H_2(t) + J\vec{S_1}.\vec{S_2}. \tag{6.3}$$

Superexchange coupling parameter J has the strength of 0.1 K which is relatively weak compared to uniaxial anisotropy term. New basis of the total Hamiltonian is written as the tensor product of two single Mn$_4$ spin states, $|M_{S_1}\rangle \otimes |M_{S_2}\rangle$, or in shorter notation $|M_{S_1}, M_{S_2}\rangle$, which are also the zeroth order eigenstates. Then, the spin wavefunction of the dimer at any time can be expanded as

$$|\Psi(t)\rangle = \sum_{M_{S_1}=-9/2}^{9/2} \sum_{M_{S_2}=-9/2}^{9/2} c_{M_{S_1},M_{S_2}}(t)|M_{S_1}, M_{S_2}\rangle. \tag{6.4}$$

6.1 Exact Time Evolution

In experiments, magnet external magnetic field is swept linearly in time. We treat the linear time dependence of field assuming small stepwise behavior with time. At each step constant magnetic field is applied for a very short time τ. Then, the field is suddenly increased for a very small amount ΔB_z. This very fast non-adiabatic change at the Hamiltonian cannot be responded by the system instantly. So, at this point, wavefunction is assumed to be remain same. Then, for the duration of τ, wavefunction evolves under the effect of time independent Hamiltonian. (Corresponding sweeping rate c is given as $\Delta B_z/\tau$.) Consequently, the unitary time evolution of the system from t to $t + \tau$ is calculated as[1]

$$|\Psi(t + \tau)\rangle = U(t + \tau, t)|\Psi(t)\rangle, \tag{6.5}$$

---

[1]We use the MATLAB program for all the numerical calculations.
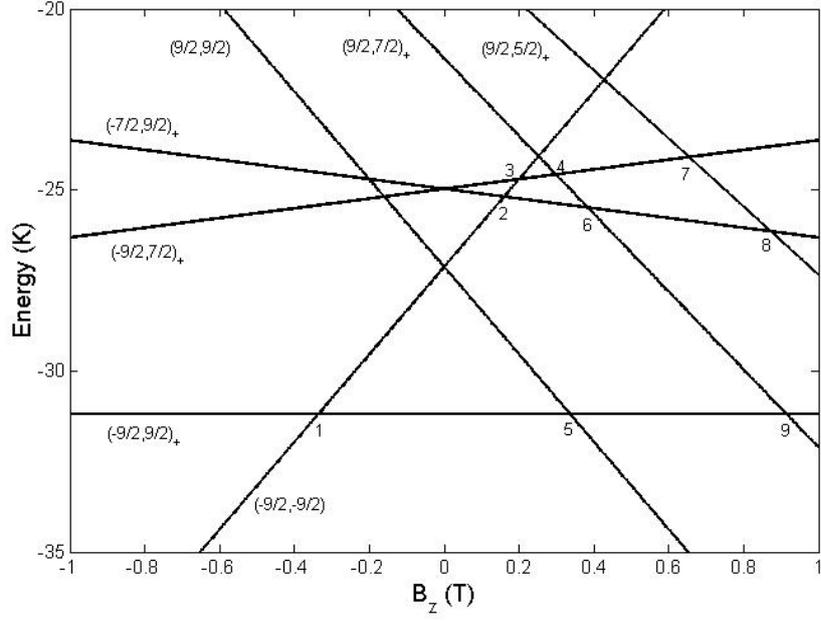
Figure 6.1: Low lying energies of the spin states as a function of the longitudinal magnetic field. Resonance points are labeled from 1 to 9.

where $U(t + \tau, t)$ is the unitary time evolution operator given as[2]

$$U(t + \tau, t) = e^{-iH(t)\tau}. \tag{6.6}$$

So, the state at n^{th} time step can be expressed in terms of the state at $(n-1)^{\text{th}}$ step

$$|\Psi(t)\rangle = |\Psi(t_0 + n\tau)\rangle = e^{-iH(t_0+(n-1)\tau)\tau}|\Psi(t_0 + (n-1)\tau)\rangle. \tag{6.7}$$

Also, applying the composition property of the unitary operators

$$U(t, t_0) = U(t, t')U(t', t_0), \tag{6.8}$$

where $t_0 < t' < t$, we can deduce the state at n^{th} step of the evolution in terms of the initial state, such that

$$|\Psi(t)\rangle = |\Psi(t_0 + n\tau)\rangle = \prod_{k=1}^{n} U(t_0 + k\tau, t_0 + (k-1)\tau)|\Psi(t_0)\rangle$$

$$= U(t_0 + n\tau, t_0)|\Psi(t_0)\rangle. \tag{6.9}$$

We first calculate the energy spectrum of the total Hamiltonian by exact diagonalization (Fig. 6.1). Then, we determine the magnetic field points, hence the times,

---

[2]In the thesis, we are using units such that the Planck constant h and the Boltzmann constant are unity.
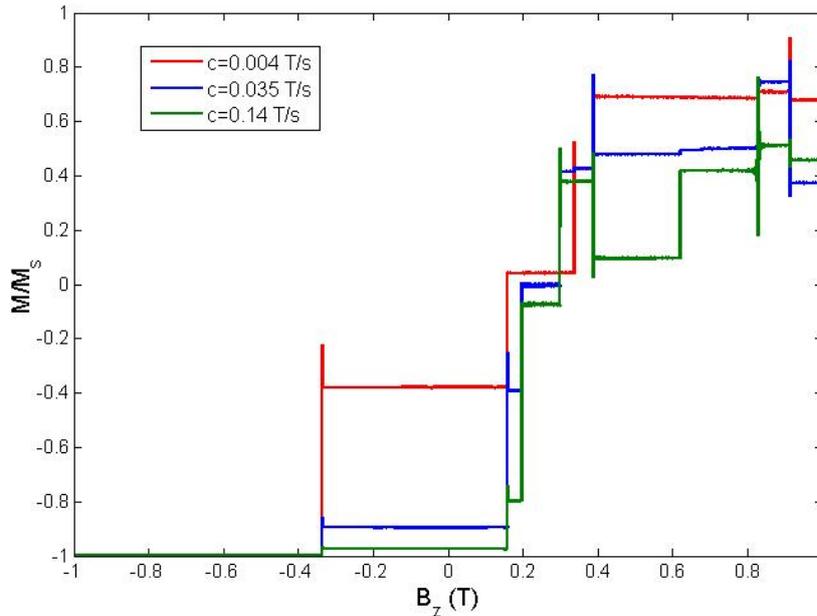
Figure 6.2: Magnetization curve as a function of longitudinal magnetic field at three different sweeping rates obtained by solving the the time-dependent Schrödinger equation.

where the different energy levels becomes very close to each other. Consequently when applying the time evolution operator, we take big magnetic field steps away from resonance points where the energy separation between the spin states is very large compared to the tunneling splitting ΔE. However, in the neighborhood of the resonance points, we take very small steps such that the corresponding change in the Zeeman energy is very small compared to the tunneling spitting ΔE.

We start the time evolution from $B_z(t_0) = -1$ T, and take the initial wavefunction as the ground state of the dimer at this field value. Magnetization M of the dimer is given by the expectation value of the z-component of the total spin operator

$$M(t) = \langle \Psi(t)|(S_{z,1} + S_{z,2})|\Psi(t)\rangle. \tag{6.10}$$

We calculate the magnetization for three different sweeping rates 0.004 T/s, 0.035, and 0.14 T/s (Fig. 6.2). Steps in the magnetization curves occur only at the resonance points labeled from 1 to 9 (Fig. 6.1). Change in sweeping rate value c effects the relative contribution of each resonance point to overall magnetization, i.e., for higher sweeping rates resonance points at the higher energy levels become important. For $c = 0.004$ T, resonance points 3, 4, 7 and 8 have no contribution to the magnetization. The effect of the sweeping rate on the magnetization tunneling is
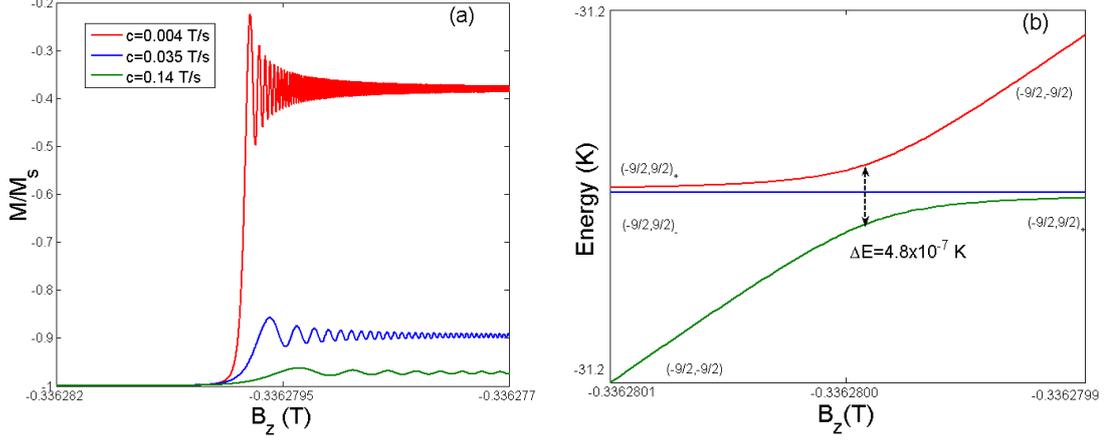
Figure 6.3: (a) Detailed view of the first jump in magnetization curve in Fig. 6.2 . Oscillations in magnetization occurs due to the precession of the spins. (b) Detailed view of the first resonance point. H_{trans} term couples the states (-9/2, -9/2), and (-9/2, 9/2)+. This causes an energy gap (tunneling splitting) between the spin states.

clearly seen at the first step position where the step height decreases with increasing sweeping rate (Fig. 6.3.a).

6.2 LZS Model

Suppression of the tunneling with increasing sweeping rate can be well understood in the picture of LZS transitions which was introduced in the previous chapter. We can consider each anti-crossing point separately as a two level problem. Time-dependent magnetic field causes two widely separated levels which are connected by a constant transverse term to become close, and then to separate. Then, according to LZS formula

$$P_{M_S \to M'_S} = 1 - \exp(-\frac{\pi(\Delta E_{M_S,M'_S})^2}{2\hbar|M_S - M'_S||\mathrm{d}B/\mathrm{d}t}),$$
(6.11)

transition probability $P_{M_S \to M'_S}$ decreases exponentially with increasing magnetic field sweeping rate. In order to check whether our results agree with LZS formalism we apply the LZS formula at each resonance point. It is assumed that there will be no change in the populations of the spin states between these points since the energy levels are well separated. First we calculated the tunneling splitting ΔE at each resonance points by exact diagonalization of the Hamiltonian and obtain the corresponding LZS transition probabilities using Eq. (6.11) at three different

35

Table 6.1: Positions of the resonance points with corresponding tunneling splittings ΔE, and tunneling probabilities P_{LZS} at three different sweeping rates.

♯	B_z(T)	Resonant levels	ΔE (10^{-5} K)	P_{LZ}		
				c=0.004 T/s	c=0.035 T/s	c=0.14 T/s
1	-0.34	$\lvert -9/2, -9/2 \rangle \rightarrow \lvert -9/2, 9/2 \rangle_+$	0.0479	0.6225	0.1054	0.0274
2	0.16	$\lvert -9/2, -9/2 \rangle \rightarrow \lvert -7/2, 9/2 \rangle_+$	0.1265	0.9978	0.5027	0.1603
3	0.20	$\lvert -9/2, -9/2 \rangle \rightarrow \lvert -9/2, 7/2 \rangle_+$	2.4869	1	1	1
4	0.30	$\lvert -9/2, 7/2 \rangle_+ \rightarrow \lvert 9/2, 7/2 \rangle_+$	0.2582	1	0.9607	0.5547
5	0.34	$\lvert -9/2, 9/2 \rangle_+ \rightarrow \lvert 9/2, 9/2 \rangle$	0.0479	0.6225	0.1054	0.0274
6	0.39	$\lvert -7/2, 9/2 \rangle_+ \rightleftharpoons \lvert 9/2, 7/2 \rangle_+$	8.3580	1	1	1
7	0.62	$\lvert -9/2, 7/2 \rangle_+ \rightarrow \lvert 9/2, 5/2 \rangle_+$	1.7340	1	1	1
8	0.83	$\lvert -7/2, 9/2 \rangle_+ \rightleftharpoons \lvert 9/2, 5/2 \rangle_+$	2.1614	1	1	1
9	0.91	$\lvert -9/2, 9/2 \rangle_+ \rightleftharpoons \lvert 9/2, 7/2 \rangle_+$	1.7262	1	1	1

sweeping rates (see Table (6.1)).

Now we explain the tunneling transition more detailed for the case where the sweeping rate $c = 0.004$ T/s. Dimer starts from the state $\lvert -9/2, -9/2 \rangle$ where $M/M_{sat} = 1$. At first resonance point LZS transition probability P_{LZS} is about 0.62 which means the probability of tunneling from the state $\lvert -9/2, -9/2 \rangle$ to the state $\lvert -9/2, 9/2 \rangle_+$ is 0.62 ($\lvert M_S, M_S' \rangle_{\pm} = 1/\sqrt{2}(\lvert M_S, M_S' \rangle \pm \lvert M_S', M_S \rangle)$). Then, the corresponding change in the magnetization value is given as $\Delta M = P_{LZS} \sum_{i=1}^{2}(M_{S,i}' - M_{S,i}) = 0.62 \times 9 = 5.58$. So, the initial dimer state follows the $1 \rightarrow 2$ path with 0.38 probability while with the 0.62 probability it follows the $1 \rightarrow 5$ path. The former path continues the $2 \rightarrow 6 \rightarrow 9$ path and ends up in $\lvert -9/2, 9/2 \rangle_+$ state without any deflection since at these resonance points tunneling probability is equal to one. The latter $1 \rightarrow 5$ path splits to two branches at point 5, one to the final state $\lvert 9/2, 9/2 \rangle$ with $P_{LZS} = 0.62$ and the other to the the point 9 with $P_{LZS} = 0.38$. The state reaching the point 9 tunnels with certainty to $\lvert 9/2, 7/2 \rangle_+$. For higher sweeping rates paths of the dimers become more complex due to inclusion of various resonance points. Between resonance points 1 and 2, we also note that the energy levels of the states $\lvert -9/2, -9/2 \rangle$ and $\lvert 9/2, 9/2 \rangle$ cross each other without any tunneling splitting. As seen in Fig. 6.4, there is a very good match between numerical solution of the Schrödinger equation and the Landau-Zener picture. In the experiment [19], five resonance points, labeling them as 1*, 2*, 3*, 4*, 5*, are attributed to the steps in the magnetization. Points 1*, 2*, 3*, and 5* match to points 1, 3,
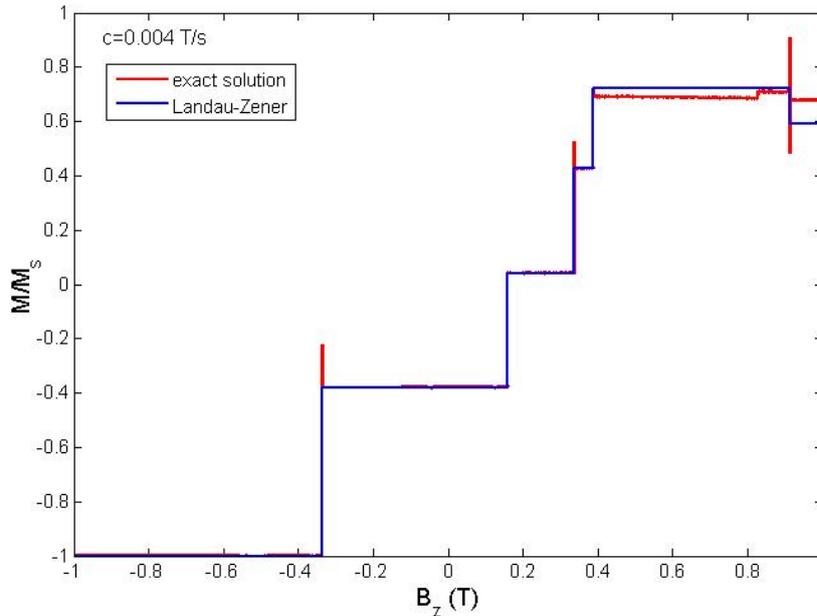
Figure 6.4: Comparison of the magnetization curves obtained by exact time evolution, and LZS method.

5, and 9 in our labeling, respectively. Transition point 4^* which corresponds to the $|-9/2, -9/2\rangle_+ \leftrightarrow |-9/2, 5/2\rangle_+$ anti-crossing is never reached within our results. It can be only observed at very high sweeping rates. Meanwhile the reason of this peak may be due to point 8 which is the $|-7/2, 9/2\rangle_+ \leftrightarrow |5/2, 9/2\rangle_+$ transition. In our results certain resonance points are very close to each other. With the effect of environmental interactions these transitions may be smeared out to give a single peak in the magnetization curve. So, it is possible that the points 2, and 3 give the peak 2^* while the points 4,5, and 6 give the peak 3^*.

We like to emphasize the two resonance points 2, and 7 ($|-9/2, -9/2\rangle \leftrightarrow |-7/2, 9/2\rangle_+$, and $|-9/2, 7/2\rangle_+ \leftrightarrow |9/2, 5/2\rangle_+$ respectively) which are overlooked by most experimental and theoretical works. These transitions involves both the tunneling of one of the Mn_4 across the barrier and the excitation (or the decaying) of the other one [3]. This type of transition is an example of spin-spin cross relaxation (SSCR) where the one-body tunnel picture is not sufficient to explain the observed transition [123]. According to our knowledge, only G.H. Kim took into account these two points [124]. However, using perturbation calculations, he argued

---

[3]Note that which Mn_4 monomer tunnels or becomes excited is a question we can't answer since they are in the entangled states and we cannot attribute any individuality to Mn_4 monomers

that transition at resonance point 2 is only possible in the presence of anisotropic exchange interaction (directional dependence of J). But according to our numerical calculations isotropic exchange coupling is sufficient to observe these SSCR type transitions.

In our result we observe a decrease in the magnetization at resonance point 5 for the highest sweeping rate and the final resonance points which did not observed in experiments. This is due to absence of the relaxation mechanisms in our model. Indeed if we look at the first resonance point in Fig. 5.2.d, although this point is well separated from all other resonant points still there is a difference between peak positions at different sweeping rates, i.e. the peaks are shifted to the right with increasing sweeping rate value. This observation also suggests the importance of interplay between measurement time (which is related to sweeping rate) and relaxation times due to system-environment interaction.

CHAPTER 7

Phonon Mediated Spin Bath Decoherence

Inspired by the observations explained in Section 5.1, we introduce a pure dephasing model where the interaction of the central two-level system with environmental spins is mediated by phonons [125]. Study of pure dephasing model is motivated by two observations. Firstly, dissipative processes where the energy exchange occurs between subsystems have typically longer time scales than pure dephasing processes [126]. Secondly, exact solubility of the model gives a more clear understanding of the decoherence process. We neglect the self-Hamiltonians of the central spin and the spin bath. In particular, we don't consider any interaction among the bath spins. We assume that low energy physics of the system is governed by the effective three-body Hamiltonian

$$H = c_z \sum_{k=1}^{N} \left[\omega_{0k} + \omega_k \left(p_k^\dagger + p_k \right) \right] s_{kz} + \sum_{k=1}^{N} \Omega_k p_k^\dagger p_k \qquad (7.1)$$

where c_z and s_{kz} are z-components of the Pauli spin operators for central two-level system and k^{th} spin of the bath, respectively. N is the total number of environmental spins. $p_k^\dagger$ and p_k are the boson creation and annihilation operators with commutation relation $[p_k, p_{k'}^\dagger] = \delta_{k,k'}$. Energy eigenvalues of the phonon bath are Ω_k, and the coupling strengths are ω_{0k} and ω_k. Our model is similar to the one proposed by Zurek where the central two level system is directly coupled to spin bath [3]. In our model this coupling occurs with the help of oscillatory modes. When ω_k and Ω_k vanish our model reduces to Zurek's. The model Hamiltonian describes a system where the central two-level system and the bath spins are coupled linearly via harmonic

oscillator displacement operators $X_k \propto (p_k^\dagger + p_k)$. Therefore, interaction among them is distance dependent and this distance is modified by some vibrational modes.

First, we solve the case where the qubit is surrounded by spins almost localized at different positions, for example at lattice points of a solid. The interaction strengths between the system and a bath spins change with the distance between them. Considering the displacement of these atomic positions as macroscopic vibrations, we model them by coherent states which are the most classical states of phonons. An atom, confined in a harmonic potential, satisfies the minimum position-momentum uncertainty when it is in a coherent state which is nothing but a Gaussian wave function displaced from the origin. Furthermore, it oscillates while preserving its shape, i.e. it remains as a coherent state. We assume that initially the system and the environment are uncorrelated so that the initial wave function can be written as a product state,

$$|\Psi(0)\rangle = (c_\uparrow|\uparrow\rangle + c_\downarrow|\downarrow\rangle) \bigotimes_{k=1}^{N} (\alpha_k|\uparrow_k\rangle + \beta_k|\downarrow_k\rangle)|\lambda_k\rangle \qquad (7.2)$$

where $|\uparrow\rangle(|\uparrow_k\rangle)$ and $|\downarrow\rangle(|\downarrow_k\rangle)$ are normalized eigenstates of $c_z(s_{kz})$ with eigenvalues +1 and -1, respectively. Expansion coefficients satisfy $|c_\uparrow|^2 + |c_\downarrow|^2 = |\alpha_k|^2 + |\beta_k|^2 = 1$ so that $|\Psi(0)\rangle$ is normalized. $|\lambda_k\rangle$ is the coherent state corresponding to the annihilation operator p_k with eigenvalue λ_k so that $p_k|\lambda_k\rangle = \lambda_k|\lambda_k\rangle$. With the help of the harmonic displacement operators $D(\alpha) = e^{\alpha p^\dagger - \alpha^* p}$, Hamiltonian can be diagonalized easily (see Appendix A for details). Applying the propagator e^{-itH}, we can calculate the time evolution of the wave function which can be written as

$$|\Psi(t)\rangle = c_\uparrow|\uparrow\rangle|B_+(t)\rangle + c_\downarrow|\downarrow\rangle|B_-(t)\rangle \qquad (7.3)$$

where

$$|B_\pm(t)\rangle = \bigotimes_{k=1}^{N} \left(\alpha_k A_k^\pm|\uparrow_k\rangle|u_k^\pm\rangle + \beta_k A_k^\mp|\downarrow_k\rangle|u_k^\mp\rangle\right). \qquad (7.4)$$

Here $|u_k^\pm\rangle$ are the coherent states with eigenvalues

$$u_k^\pm = (\lambda_k \pm \frac{\omega_k}{\Omega_k})e^{-it\Omega_k} \mp \frac{\omega_k}{\Omega_k}, \qquad (7.5)$$

and

$$A_k^\pm = \quad e^{i\frac{\omega_k^2}{\Omega_k}\left(t - \frac{\sin(\Omega_k t)}{\Omega_k}\right)}e^{\mp it\omega_{0k}}$$
$$\times e^{\mp i\frac{\omega_k}{\Omega_k}(\text{Re}[\lambda_k]\sin(\Omega_k t) + \text{Im}[\lambda_k](1-\cos(\Omega_k t)))}. \qquad (7.6)$$

Total density matrix is given by $\rho = |\Psi(t)\rangle\langle\Psi(t)|$. Reduced density matrix of the central system ρ_c is obtained by tracing over all the environmental degrees of freedom as $\rho_c = Tr_{bath}\rho$. In c_z-basis, the reduced density matrix is given by

$$\rho_c = \begin{pmatrix} |c_\uparrow|^2 & c_\uparrow c_\downarrow^* r \\ c_\uparrow^* c_\downarrow r^* & |c_\downarrow|^2 \end{pmatrix} \tag{7.7}$$

Magnitude of the off-diagonal matrix element is determined by the decoherence factor

$$r(t) = \prod_{k=1}^{N}(|\alpha_k|^2 A_k^{-*} A_k^+ \langle u_k^-|u_k^+\rangle + |\beta_k|^2 A_k^{+*} A_k^- \langle u_k^+|u_k^-\rangle) \tag{7.8}$$

which can be written more explicitly as

$$r(t) = \prod_{k=1}^{N} e^{-4\frac{\omega_k^2}{\Omega_k^2}(1-\cos(\Omega_k t))} \quad (|\alpha_k|^2 e^{-i2\omega_{0k}t - i4\frac{\omega_k}{\Omega_k}(\text{Re}[\lambda_k]\sin(\Omega_k t)+\text{Im}[\lambda_k](1-\cos(\Omega_k t)))}$$

$$+|\beta_k|^2 e^{i2\omega_{0k}t + i4\frac{\omega_k}{\Omega_k}(\text{Re}[\lambda_k]\sin(\Omega_k t)+\text{Im}[\lambda_k](1-\cos(\Omega_k t)))}). \tag{7.9}$$

At $t = 0$, $r = 1$ and as t increases, in general, it decays to zero which means that interference of the states $|\uparrow\rangle$ and $|\downarrow\rangle$ is totally suppressed. At short enough times we can expand the trigonometric functions by treating $\Omega_k t$'s as small parameters to obtain

$$r(t) \approx \prod_{k=1}^{N} e^{-2\omega_k^2 t^2} \quad (|\alpha_k|^2 e^{-it(4\omega_k \text{Re}[\lambda_k]+2\omega_{0k})}$$

$$+|\beta_k|^2 e^{it(4\omega_k \text{Re}[\lambda_k]+2\omega_{0k})}). \tag{7.10}$$

If either the coupling strengths ω_k's and ω_{0k}'s or coherent state eigenvalues λ_k's are random enough, the second factor in the product leads to further suppression of the coherence factor so that r decays in Gaussian form for large N [71],

$$|r(t)| \approx e^{-t^2 \sum_k (8|\alpha_k|^2|\beta_k|^2(2\omega_k \text{Re}[\lambda_k]+\omega_{0k})^2+2\omega_k^2)}. \tag{7.11}$$

Therefore, phonon energies do not play any role for short time decoherence of the central system. The decoherence time is determined by the coupling constants and the initial configurations of the phonons and spin bath states. It is interesting to note that even if all the bath spins are polarized in one direction, i.e. $|\alpha_k|^2 = 1$, system still loses its coherence. This behavior is a result of presence of the phonons in the environment. It is also interesting that phonon state eigenvalues (λ_k's) do not

affect the decoherence time in this case. It is obvious that in the limit of $\Omega_k \to 0$ and $\omega_k \to 0$, our Hamiltonian is reduced to Zurek's model where decoherence is due to direct spin-spin interactions only without phonon contribution. In this case initial configuration of the spin bath becomes crucial.

Another interesting case is the $\Omega_k/\omega_k \to \infty$ limit where

$$r(t) = \prod_{k=1}^{N} (|\alpha_k|^2 e^{-i2\omega_{0k}t} + |\beta_k|^2 e^{i2\omega_{0k}t}). \tag{7.12}$$

Here, decoherence factor $r(t)$ depends on the initial configuration of bath spins only and it becomes independent of the initial phonon state eigenvalues. Since the separation of energy levels of phonons becomes very high, phonon states do not change in time and remain uncorrelated to system and bath spins.

Now, we analyze the case where phonons are in a thermal equilibrium rather than a coherent state. Such a situation can physically be realized when the atoms carrying bath spins are brought in contact with a heat bath to thermalize before $t = 0$. For thermal states phonon density matrix is given by

$$\rho_p(0) = \bigotimes_k (1 - e^{-\frac{\Omega_k}{T}}) \sum_{n_k=0}^{\infty} e^{-\frac{\Omega_k n_k}{T}} |n_k\rangle\langle n_k|. \tag{7.13}$$

We assume that the bath spins are in a separable state at $t = 0$ as before. Since in the Hamiltonian there are no intra-bath terms for the spins, heat bath thermalizing the phonons will simply randomize the initial spin directions. As we shall discuss below, if bath spins have individual energy levels for up and down configurations, heat bath will determine the initial occupation numbers for the two possible states in accordance with the Gibbs factors. Time evolution of the total density matrix is given by $\rho(t) = e^{-iHt}\rho(0)e^{iHt}$. Using the over-completeness relation

$$\mathbf{1} = \frac{1}{\pi} \int d^2\lambda |\lambda\rangle\langle\lambda|, \tag{7.14}$$

and the number state representation of coherent states

$$\langle n|\lambda\rangle = e^{-|\lambda|^2/2} \frac{\lambda^n}{\sqrt{n!}}, \tag{7.15}$$

it is possible to calculate the reduced density matrix of the central system (see Appendix B for details). In this case decoherence factor becomes
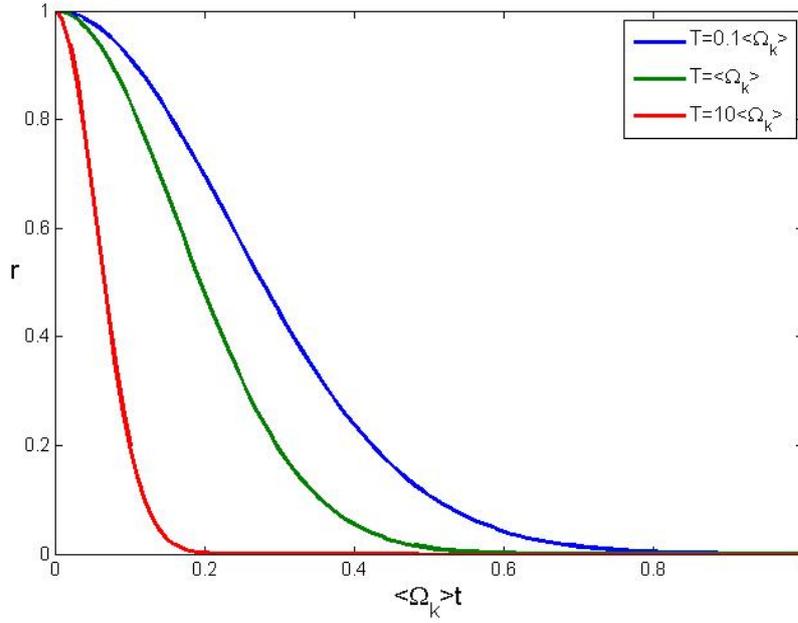
Figure 7.1: Decoherence factor at three different temperatures. Interaction parameters and phonon frequencies are assumed to be in normal distribution with variance to average ratios $\frac{\sigma}{<>} = 0.1$. Also, we take $< \omega_{0k} > = 0.1 < \Omega_k >$ and $< \omega_k > = 0.2 < \Omega_k >$.

$$r(t) = \prod_{k=1}^{N} e^{-4\frac{\omega_k^2}{\Omega_k^2}(1-\cos(\Omega_k t))\coth(\frac{\Omega_k}{2T})}$$
$$\times (|\alpha_k|^2 e^{-i2\omega_{0k}t} + |\beta_k|^2 e^{i2\omega_{0k}t}). \tag{7.16}$$

We first note that for $\Omega_k/T \to \infty$, Eq. (7.16) and Eq. (7.9) become identical provided that $\lambda_k = 0$. This is a consistency check for two phonon states, coherent states and thermal states, that we have discussed because at low temperatures thermal state approaches the ground state of the harmonic oscillators which are nothing but the coherent states with vanishing eigenvalues.

According to Eq. (7.16), decoherence factor has two contributions, coming from phonons and spins. The two mechanisms act simultaneously in decoherence of the central spin. Depending upon the interaction strengths, one of them can become the dominant mechanism. At very low temperatures $T \ll \Omega_k$, where the hyperbolic cotangent term is approximately unity, the first term becomes independent of Ω_k values provided that t is small enough. For large temperatures $T \gg \Omega_k$, decoherence factor becomes an exponentially decaying function of T. It is possible to generalize the model Hamiltonian by adding a s_{kz}-dependent intra-bath term for individual spins. In this case the heat bath will not only thermalize the phonons but also

it will determine the $|\alpha_k|^2/|\beta_k|^2$ ratio. For example, at very large temperatures the ratio will tend to unity and hence the spin bath will have a more important contribution to decoherence in comparison to lower temperatures.

7.1 Entangled Environment

Interactions within the environment can greatly influence the dynamics of the central system. It is has been shown that intra-environmental couplings can increase the coherence time of the qubit [84, 127]. This result can be interpreted in terms of entanglement sharing between central system and environment. It has been proven that a quantum system entangled with another one restricts its possible entanglement with a third system, this has been referred to as *entanglement monogamy* [128, 129, 130]. This effect is also generalized to n qubit system [131]. So, intra-bath interactions leading to entanglement between them limits their entanglement to central system. In result, decoherence effect of the bath reduces. For higher dimensional discrete systems, qudits, applicability of this monogamy relation is an open question [132]. However, for continuous variable systems with infinite dimensional Hilbert spaces, it is shown that the monogamy property is satisfied for Gaussian states [133]. Since coherent states are also the special case of Gaussian sates, they also exhibit entanglement monogamy.

Accordingly, we investigate the effect of intra-bath entanglement on the decoherence time of the central system. We compare the two cases where the initial bath states are

$$|B_E(0)\rangle = \bigotimes_{k=1}^{N} (\alpha_k|\uparrow_k\rangle|\lambda_{k1}\rangle + \beta_k|\downarrow_k\rangle|\lambda_{k2}\rangle) \tag{7.17}$$

for the entangled bath, and

$$|B_S(0)\rangle = \bigotimes_{k=1}^{N} \left((\alpha_k|\uparrow_k\rangle + \beta_k|\downarrow_k\rangle) \frac{1}{\sqrt{N_k}} (|\lambda_{k1}\rangle + |\lambda_{k2}\rangle) \right) \tag{7.18}$$

for the separated baths. Here N_k are the normalization constants of the phonon states. Repeating the previous calculations for these two cases, we find the following short time ($\Omega_k t \ll 1$) decoherence factors

$$|r_S(t)| \approx e^{-t^2 \sum_k (2+\lambda_{k-}^2)\omega_k^2 + 8|\alpha_k|^2|\beta_k|^2(\omega_{0k}+\omega_k\lambda_{k+})^2}, \tag{7.19}$$

$$|r_E(t)| \approx e^{-t^2 \sum_k 2\omega_k^2 + 8|\alpha_k|^2|\beta_k|^2(\omega_{0k}+\omega_k\lambda_{k+})^2}, \tag{7.20}$$

for separated bath and entangled bath, respectively. Here $\lambda_{k\pm} = \lambda_{k1} \pm \lambda_{k2}$. Defining the variance of Gaussian as a decoherence time τ, we find that

$$\frac{1}{\tau_S^2} = \frac{1}{\tau_E^2} + 2\sum_{k=1}^{N} \omega_k^2 \lambda_{k-}^2. \tag{7.21}$$

We see that decoherence time for entangled bath, τ_E, is always longer than decoherence time for separated bath, τ_S. Note that amount of entanglement in $|B_E(0)\rangle$ is proportional to magnitude of λ_{k-} since $|\lambda_{k1}\rangle$ and $|\lambda_{k2}\rangle$ become more orthogonal to each other with increasing magnitude of λ_{k-}. According to Eq. (7.21), difference between τ_E and τ_S also increases with λ_{k-}^2. This means that as the bath spin and the corresponding phonon become entangled, central system becomes less decoherent. Thus, entanglement of environment to central system becomes restricted. This result suggests that entanglement distributed over three parties composed of two qubits and one coherent phonon mode also exhibits monogamy property. Consequently, it might be be possible to extend the idea of entanglement monogamy that exist separately within qubits and within Gaussian states to a compound systems made of both types of states.

7.2   Decoherence of Entangled Central System

Now we apply our decoherence model to study the entanglement dynamics of central bipartite two-level system. During the decoherence process, as the central system becomes entangled with the environment, they lose their entanglement with each other. Hence entanglement measure quantifying the quantum correlations within the central system can be used to parameterize the decoherence. We examine the behaviors of four Bell states, and we choose the concurrence as an entanglement measure.

We compare two different environment models: common spin bath, and two separate spin baths. Former model can be realized when two spins are not well separated from each other. Thus, they interact collectively with common spin bath.

However, when they are well isolated in space from each other, the latter model is the reasonable one.

7.2.1 Common Spin Bath

First we consider the two spin interaction with common environment. Total Hamiltonian of the system is given by

$$H = (c_{1z} + c_{2z}) \sum_{k=1}^{N} \left[\omega_{0k} + \omega_k \left(p_k^\dagger + p_k \right) \right] s_{kz} + \sum_{k=1}^{N} \Omega_k p_k^\dagger p_k. \tag{7.22}$$

Starting from the initial state of separated central system and environment, time evolution of the reduced density matrix of central spin pair is calculated as

$$\rho(t) = \begin{pmatrix} \rho_{0,0} & \rho_{0,1}r & \rho_{0,2}r & \rho_{0,3}R \\ \rho_{1,0}r^* & \rho_{1,1} & \rho_{1,2} & \rho_{1,3}r \\ \rho_{2,0}r^* & \rho_{2,1} & \rho_{2,2} & \rho_{2,3}r \\ \rho_{3,0}R^* & \rho_{3,1}r^* & \rho_{3,2}r^* & \rho_{3,3} \end{pmatrix}, \tag{7.23}$$

where $r(t)$ is the same decoherence factor in Eq. (7.9) while $R(t)$ is given by applying the transformations $\omega_k \to 2\omega_k$ and $\omega_{0k} \to 2\omega_{0k}$ in Eq. (7.9). Then, following the assumptions in deriving Eq. (7.11), we can express the approximate magnitude of the decoherence factor $R(t)$ as

$$|R(t)| \approx e^{-t^2 \sum_k (32|\alpha_k|^2 |\beta_k|^2 (2\omega_k \mathrm{Re}[\lambda_k] + \omega_{0k})^2 + 8\omega_k^2)} \approx |r(t)|^4. \tag{7.24}$$

We note that the terms $\rho_{1,2}$ and $\rho_{1,2}$ corresponding to interference of $|\uparrow\downarrow\rangle$ and $|\downarrow\uparrow\rangle$ states do not decay and remain constant in time. This is an example of decoherence free subspace where symmetric coupling to the environment leads to a certain robust states against decoherence [134, 135, 35].

Concurrence of the density matrix ρ can be calculated by following the discussion in Section 3.2. Spin-flipped density matrix $\tilde{\rho}$ is given by

$$\tilde{\rho}(t) = \begin{pmatrix} \rho_{3,3} & -\rho_{2,3}r & -\rho_{1,3}r & \rho_{0,3}R \\ -\rho_{3,2}r^* & \rho_{2,2} & \rho_{1,2} & -\rho_{0,2}r \\ -\rho_{3,1}r^* & \rho_{2,1} & \rho_{1,1} & -\rho_{0,1}r \\ \rho_{3,0}R^* & -\rho_{1,0}r^* & -\rho_{1,0}r^* & \rho_{0,0} \end{pmatrix}. \tag{7.25}$$

46

Accordingly, concurrences of the four Bell states are calculated as

$$C_{\Psi_+} = C_{\Psi_-} = |R_c| \approx |r|^4$$

$$C_{\Phi_+} = C_{\Phi_-} = 1. \tag{7.26}$$

Thus, we obtain two by two grouping of the Bell states in terms of the concurrence. In the first group, entanglement of the system decays more faster than the decoherence factor, while the second group, which constitutes the decoherence free subspace, remain always entangled.

7.2.2 Separate Spin Baths

Now we consider the second case where each spin of the central pair interacts locally only with its own spin bath. Corresponding Hamiltonian follows as

$$H = c_{1z} \sum_{k=1}^{N} \left[\omega_{0k} + \omega_k \left(p_{1k}^\dagger + p_{1k} \right) \right] s_{1kz} + \sum_{k=1}^{N} \Omega_k p_{1k}^\dagger p_{1k}$$

$$+ c_{2z} \sum_{k=1}^{N} \left[\omega_{0k} + \omega_k \left(p_{2k}^\dagger + p_{2k} \right) \right] s_{2kz} + \sum_{k=1}^{N} \Omega_k p_{2k}^\dagger p_{2k}. \tag{7.27}$$

Again starting from initially separate states, time evolution of the reduced density matrix turns out to be

$$\rho(t) = \begin{pmatrix} \rho_{0,0} & \rho_{0,1} r & \rho_{0,2} r & \rho_{0,3} r^2 \\ \rho_{1,0} r^* & \rho_{1,1} & \rho_{1,2} |r|^2 & \rho_{1,3} r \\ \rho_{2,0} r^* & \rho_{2,1} |r|^2 & \rho_{2,2} & \rho_{2,3} r \\ \rho_{3,0} r^{*2} & \rho_{3,1} r^* & \rho_{3,2} r^* \gamma & \rho_{3,3} \end{pmatrix}, \tag{7.28}$$

where the decoherence factor $r(t)$ is again same with Eq. (7.9). In separate bath case all the states are affected by decoherence. Spin-flipped density matrix $\tilde{\rho}$ is given by

$$\tilde{\rho}(t) = \begin{pmatrix} \rho_{3,3} & -\rho_{2,3} r & -\rho_{1,3} r & \rho_{0,3} r^2 \\ -\rho_{3,2} r^* & \rho_{2,2} & \rho_{1,2} |r|^2 & -\rho_{0,2} r \\ -\rho_{3,1} r^* & \rho_{2,1} |r|^2 & \rho_{1,1} & -\rho_{0,1} r \\ \rho_{3,0} r^{*2} & -\rho_{1,0} r^* & -\rho_{1,0} r^* & \rho_{0,0} \end{pmatrix}. \tag{7.29}$$

Corresponding concurrence have the same value for all Bell states

$$C = |r|^2. \tag{7.30}$$

47

To sum up, we observe that presence of the decoherence free subspace in common spin bath leads to a classification of the Bell states according to their entanglement decay under decoherence. However, in separate bath case, there is no such classification of Bell states, and they all loose their entanglement in the same way. We also note that fragile Bell states of the common bath loose their entanglement much faster than the states in separate baths.

CHAPTER 8

Dephasing in Entangled Qutrits

Recently, effect of dephasing on entangled qutrits have been studied in terms of classical noise [136, 137]. In these models stochastic fluctuations have been added to the Hamiltonian of the system. This result in unitary evolution of the system and does not create any system-environment entanglement. Changes in state of the system can be completely undone with local operations. The loss of coherence can show itself only in ensemble, i.e.; in the form of ensemble average over a different realizations of particular noise processes. At the level of reduced density matrix formalism both cases, entanglement with environment and classical noise, are identical. However, the latter is called as *fake decoherence* and it does not correspond to a decoherence process in usual sense which is identified as delocalization of phase relations for individual systems [138]. Decoherence on entangled qutrits, using both canonical models [139] and quantum channels [140], have been investigated recently.

In this chapter we analyze these two cases, classical noise, and decoherence, including both local and collective interactions. Then, we study time evolution of Horodecki's bound entangled state and Bell like states [141].

8.1 Classical Stochastic Noise

We consider the following Hamiltonian

$$H = -\frac{1}{2}\mu \left[B(t)(c_{zA} + c_{zB}) + b_A(t)c_{zA} + b_B(t)c_{zB} \right],$$
(8.1)

which is in the same form as Hamiltonian in [142] except here the spin operator c_z^i corresponds the z component of the three level spin

$$c_z^{A,B} = \begin{pmatrix} 0 & 0 & 0 \\ 0 & 1 & 0 \\ 0 & 0 & 2 \end{pmatrix}. \tag{8.2}$$

Here, μ is the gyromagnetic ratio and $B(t)$, $b_A(t)$, and b_B are stochastic fields leading to statistical independent Markov processes satisfying

$$\langle B(t) \rangle = 0, \tag{8.3}$$

$$\langle B(t)B(t') \rangle = \frac{\Gamma}{\mu^2} \delta(t - t'), \tag{8.4}$$

$$\langle b_i(t) \rangle = 0, \tag{8.5}$$

$$\langle b_i(t)b_i(t') \rangle = \frac{\Gamma_i}{\mu^2} \delta(t - t'), \tag{8.6}$$

where $\langle ... \rangle$ stands for ensemble average, and $i = A, B$. Γ and Γ_i are dephasing rates due to $B(t)$ and $b_i(t)$, respectively.

We use the standard two-qutrit bases such that $|n\rangle_{AB} = |m_A m_B (mod(3))\rangle_{AB} = |m_A\, m_B\rangle_{AB}$. Time evolution of the system's density matrix can be evaluated as

$$\rho(t) = \langle U(t)\rho(0)U^\dagger(t) \rangle \tag{8.7}$$

where ensemble average is taken over three noise fields and $U(t)$ is time evolution operator $U(t) = \exp\left[-i \int_0^t dt' H(t')\right]$.

8.1.1   Collective Dephasing

In the absence of local noise $b_i = 0$, qutrits interact only with a common stochastic field. In this case elements of the reduced density matrix are given by

$$\rho_{m_A m_B, m'_A m'_B}(t) = \rho_{m_A m_B, m'_A m'_B}(0)\langle e^{i\frac{\mu}{2}(m_A + m_B - m'_A - m'_B)\int_0^t dt' B(t')} \rangle, \tag{8.8}$$

$$= \rho_{m_A m_B, m'_A m'_B}(0)e^{-\frac{\mu^2(m_A + m_B - m'_A - m'_B)^2}{8}\int_0^t \int_0^t dt' dt'' \langle B(t')B(t'') \rangle}, \tag{8.9}$$

$$= \rho_{m_A m_B, m'_A m'_B}(0)e^{-\frac{(m_A + m_B - m'_A - m'_B)^2}{8}t\Gamma}. \tag{8.10}$$

Density matrix can be written more explicitly as

$$\rho(t) = \begin{pmatrix} \rho_{0,0} & \rho_{0,1}\gamma & \rho_{0,2}\gamma^4 & \rho_{0,3}\gamma & \rho_{0,4}\gamma^4 & \rho_{0,5}\gamma^9 & \rho_{0,6}\gamma^4 & \rho_{0,7}\gamma^9 & \rho_{0,8}\gamma^{16} \\ \rho_{1,0}\gamma & \rho_{1,1} & \rho_{1,2}\gamma & \rho_{1,3} & \rho_{1,4}\gamma & \rho_{1,5}\gamma^4 & \rho_{1,6}\gamma & \rho_{1,7}\gamma^4 & \rho_{1,8}\gamma^9 \\ \rho_{2,0}\gamma^4 & \rho_{2,1}\gamma & \rho_{2,2} & \rho_{2,3}\gamma & \rho_{2,4} & \rho_{2,5}\gamma & \rho_{2,6} & \rho_{2,7}\gamma & \rho_{2,8}\gamma^4 \\ \rho_{3,0}\gamma & \rho_{3,1} & \rho_{3,2}\gamma & \rho_{3,3} & \rho_{3,4}\gamma & \rho_{3,5}\gamma^4 & \rho_{3,6}\gamma & \rho_{3,7}\gamma^4 & \rho_{3,8}\gamma^9 \\ \rho_{4,0}\gamma^4 & \rho_{4,1}\gamma & \rho_{4,2} & \rho_{4,3}\gamma & \rho_{4,4} & \rho_{4,5}\gamma & \rho_{4,6} & \rho_{4,7}\gamma & \rho_{4,8}\gamma^4 \\ \rho_{5,0}\gamma^9 & \rho_{5,1}\gamma^4 & \rho_{5,2}\gamma & \rho_{5,3}\gamma^4 & \rho_{5,4}\gamma & \rho_{5,5} & \rho_{5,6}\gamma & \rho_{5,7} & \rho_{5,8}\gamma \\ \rho_{6,0}\gamma^4 & \rho_{6,1}\gamma & \rho_{6,2} & \rho_{6,3}\gamma & \rho_{6,4} & \rho_{6,5}\gamma & \rho_{6,6} & \rho_{6,7}\gamma & \rho_{6,8}\gamma^4 \\ \rho_{7,0}\gamma^9 & \rho_{7,1}\gamma^4 & \rho_{7,2}\gamma & \rho_{7,3}\gamma^4 & \rho_{7,4}\gamma & \rho_{7,5} & \rho_{7,6}\gamma & \rho_{7,7} & \rho_{7,8}\gamma \\ \rho_{8,0}\gamma^{16} & \rho_{8,1}\gamma^9 & \rho_{8,2}\gamma^4 & \rho_{8,3}\gamma^9 & \rho_{8,4}\gamma^4 & \rho_{8,5}\gamma & \rho_{8,6}\gamma^4 & \rho_{8,7}\gamma & \rho_{8,8} \end{pmatrix}, \tag{8.11}$$

where $\gamma = e^{-t\Gamma/8}$. We obtain four different dephasing factors: γ, γ^4, γ^9, and γ^{16}. Most fragile states correspond to ones with $\rho_{0,8}$ and $\rho_{8,0}$ terms. We also see that some terms are not affected by the noise. These interference terms are robust to phase damping due to their symmetric coupling to noise field. Components of the robust superpositions are degenerate states. Therefore, their superposition is also the eigenstate of the Hamiltonian and they stay unchanged in the course of time evolution.

8.1.2   Multilocal Dephasing

Now we consider the case where the collective dephasing field is absent while both local noises affect the qutrits. Then, time evolution of the density matrix is evaluated as

$$\rho_{m_A m_B, m'_A m'_B}(t) = \rho_{m_A m_B, m'_A m'_B}(0)\langle e^{i\frac{\mu}{2}\int_0^t \left[b_A(t')(m_A - m'_A)(t') + b_B(t')(m_B - m'_B)\right]dt'}\rangle \tag{8.12}$$

$$= \rho_{m_A m_B, m'_A m'_B}(0)e^{-\frac{(m_A - m'_A)^2}{8}t\Gamma_A}e^{-\frac{(m_B - m'_B)^2}{8}t\Gamma_B}, \tag{8.13}$$

$$\rho(t) = \begin{pmatrix} \rho_{0,0} & \rho_{0,1}\gamma_B & \rho_{0,2}\gamma_B^4 & \rho_{0,3}\gamma_A & \rho_{0,4}\gamma_A\gamma_B & \rho_{0,5}\gamma_A\gamma_A^4 & \rho_{0,6}\gamma_A^4 & \rho_{0,7}\gamma_A^4\gamma_B & \rho_{0,8}\gamma_A^4\gamma_A^4 \\ \rho_{1,0}\gamma_B & \rho_{1,1} & \rho_{1,2}\gamma_B & \rho_{1,3}\gamma_A\gamma_B & \rho_{1,4}\gamma_A & \rho_{1,5}\gamma_A\gamma_B & \rho_{1,6}\gamma_A^4\gamma_B & \rho_{1,7}\gamma_A^4 & \rho_{1,8}\gamma_A^4\gamma_B \\ \rho_{2,0}\gamma_B^4 & \rho_{2,1}\gamma_B & \rho_{2,2} & \rho_{2,3}\gamma_A\gamma_A^4 & \rho_{2,4}\gamma_A\gamma_B & \rho_{2,5}\gamma_A & \rho_{2,6}\gamma_A^4\gamma_B^4 & \rho_{2,7}\gamma_A^4\gamma_B & \rho_{2,8}\gamma_A^4 \\ \rho_{3,0}\gamma_A & \rho_{3,1}\gamma_A\gamma_B & \rho_{3,2}\gamma_A\gamma_B^4 & \rho_{3,3} & \rho_{3,4}\gamma_B & \rho_{3,5}\gamma_B^4 & \rho_{3,6}\gamma_A & \rho_{3,7}\gamma_A\gamma_B & \rho_{3,8}\gamma_A\gamma_B^4 \\ \rho_{4,0}\gamma_A\gamma_B & \rho_{4,1}\gamma_A & \rho_{4,2}\gamma_A\gamma_B & \rho_{4,3}\gamma_B & \rho_{4,4} & \rho_{4,5}\gamma_B & \rho_{4,6}\gamma_A\gamma_B & \rho_{4,7}\gamma_A & \rho_{4,8}\gamma_A\gamma_B \\ \rho_{5,0}\gamma_A\gamma_B^4 & \rho_{5,1}\gamma_A\gamma_B & \rho_{5,2}\gamma_A & \rho_{5,3}\gamma_B^4 & \rho_{5,4}\gamma_B & \rho_{5,5} & \rho_{5,6}\gamma_A\gamma_B^4 & \rho_{5,7}\gamma_A\gamma_B & \rho_{5,8}\gamma_A \\ \rho_{6,0}\gamma_A^4 & \rho_{6,1}\gamma_A^4\gamma_B & \rho_{6,2}\gamma_A^4\gamma_B^4 & \rho_{6,3}\gamma_A & \rho_{6,4}\gamma_A\gamma_B & \rho_{6,5}\gamma_A\gamma_B^4 & \rho_{6,6} & \rho_{6,7}\gamma_B & \rho_{6,8}\gamma_B^4 \\ \rho_{7,0}\gamma_A^4\gamma_B & \rho_{7,1}\gamma_A^4 & \rho_{7,2}\gamma_A^4\gamma_B & \rho_{7,3}\gamma_A\gamma_B & \rho_{7,4}\gamma_A & \rho_{7,5}\gamma_A\gamma_B & \rho_{7,6}\gamma_B & \rho_{7,7} & \rho_{7,8}\gamma_B \\ \rho_{8,0}\gamma_A^4\gamma_B^4 & \rho_{8,1}\gamma_A^4\gamma_B & \rho_{8,2}\gamma_A^4 & \rho_{8,3}\gamma_A\gamma_B & \rho_{8,4}\gamma_A\gamma_B & \rho_{8,5}\gamma_A & \rho_{8,6}\gamma_B^4 & \rho_{8,7}\gamma_B & \rho_{8,8} \end{pmatrix},$$

$$\tag{8.14}$$

where $\gamma_i = e^{-t\Gamma_i/8}$. All of the off-diagonal terms in density matrix decay in time. So, we do not observe any robust states. Most fragile states are the ones containing $\rho_{0,8}$, $\rho_{8,0}$, $\rho_{2,6}$, and $\rho_{6,2}$.

8.2 Spin Bath Environment

8.2.1 Common Spin Bath

Now we consider pure dephasing model where a central two qutrit system is surrounded by quantum environment represented by a collection of spin-$\frac{1}{2}$ particles. Total Hamiltonian is given as

$$H = (c_{zA} + c_{zB}) \sum_{k=1}^{N} \omega_k s_{kz}, \tag{8.15}$$

where s_{kz} are z-components of Pauli matrices for k^{th} bath spin, N is the total number of bath spins, and ω_k are coupling parameters. Initial state of the environment is considered as

$$|\psi_{env}\rangle = \bigotimes_{k=1}^{N} (\alpha_k |\uparrow\rangle_k + \beta_k |\downarrow\rangle_k), \tag{8.16}$$

where $|\uparrow\rangle_k$ are $|\downarrow\rangle_k$ eigenstates of s_{kz} with eigenvalues $+1$ and -1, respectively, and $|\alpha_k|^2 + |\beta_k|^2 = 1$. Assuming that initially central system and environment start from product state, reduced density matrix of the central system evolves as following

$$\rho_{m_A m_B, m'_A m'_B}(t) = \rho_{m_A m_B, m'_A m'_B}(0) \prod_{k=1}^{N} (|\alpha_k|^2 \, e^{it\omega_k(m_A + m_B - m'_A - m'_B)}$$
$$+ |\beta_k|^2 \, e^{-it\omega_k(m_A + m_B - m'_A - m'_B)}). \tag{8.17}$$

For large N, if the coupling strengths ω_k's are random enough above expression becomes

$$|\rho_{m_A m_B, m'_A m'_B}(t)| = \rho_{m_A m_B, m'_A m'_B}(0) e^{-2t^2 \sum_k^N |\alpha_k|^2 |\beta_k|^2 \omega_k^2 (m_A + m_B - m'_A - m'_B)^2}. \tag{8.18}$$

Introducing $\gamma_c = e^{-2t^2 \sum_k^N |\alpha_k|^2 |\beta_k|^2 \omega_k^2}$, we see that above equation is exactly in the same form up to a phase constant as density matrix obtained from collective dephasing due to a classical noise in Eq. (8.11). We will obtain same resemblance also for multilocal dephasing case. So, most of the conclusions deduced from density matrix formalism will be similar for quantum and classical noises. However, we should also emphasize one major distinction between them. While the off-diagonal elements decay in exponential form for the classical noise, Gaussian decay is observed for the quantum decoherence. Therefore, initially, the classical noise leads to more rapid dephasing with respect to quantum environment, while in time the latter becomes more dominant.

8.2.2 Separate Spin Baths

Now we consider a model where two qutrits interact with their own separate environments

$$H = c_{zA} \sum_{k=1}^{N_A} \omega_{kA} s_{zkA} + c_{zB} \sum_{k=1}^{N_B} \omega_{kB} s_{kzB}, \tag{8.19}$$

where s_{kzi} are z-components of Pauli matrices for k^{th} spin of ith bath composed of N_i number of spins, and ω_{ki} are corresponding coupling parameters. Initial bath states are given by

$$|\psi_{env}\rangle = \bigotimes_{i=1}^{2} |\psi_{s,i}\rangle, \tag{8.20}$$

with

$$|\psi_{s,i}\rangle = \bigotimes_{k=1}^{N_i} (\alpha_{ki} |\uparrow\rangle_{ki} + \beta_{ki} |\downarrow\rangle_{ki}). \tag{8.21}$$

Starting from unentangled pure product states of qutrits and bath spins we obtain the following reduced density matrix

$$\rho_{m_A m_B, m'_A m'_B}(t) = \rho_{m_A m_B, m'_A m'_B}(0) \prod_{k=1}^{N_A} \left(|\alpha_{kA}|^2 e^{it\omega_{kA}(m_A - m'_A)} + |\beta_{kA}|^2 e^{-it\omega_{kA}(m_A - m'_A)} \right)$$
$$\times \prod_{k=1}^{N_B} \left(|\alpha_{kB}|^2 e^{it\omega_{kB}(m_B - m'_B)} + |\beta_{kB}|^2 e^{-it\omega_{kB}(m_B - m'_B)} \right). \tag{8.22}$$

Approximation used to obtain Eq. (8.23) can be applied to get

$$|\rho_{m_A m_B, m'_A m'_B}(t)| = \rho_{m_A m_B, m'_A m'_B}(0)$$
$$\times e^{-2t^2 \left(\sum_k^{N_A} |\alpha_{kA}|^2 |\beta_{kA}|^2 \omega_{kA}^2 (m_A - m'_A)^2 + \sum_k^{N_B} |\alpha_{kB}|^2 |\beta_{kB}|^2 \omega_{kB}^2 (m_B - m'_B)^2 \right)} \tag{8.23}$$

Now introducing $\gamma_{d,i} = e^{-2t^2 \sum_k^{N_i} |\alpha_{ki}|^2 |\beta_{ki}|^2 \omega_{ki}^2}$, we obtain the same density matrix as Eq. (8.14).

We see that density matrix formalism gives us equivalent results for both dephasing processes which have fundamentally different physical origin. This result is true for both collective and local interactions. So, in the rest of chapter we will focus on only quantum decoherence case and compare various entangled qutrit states for common and separate bath cases.

8.3 Qutrit Bell-like States

There are nine Bell-like states for qutrits that can be grouped into three parts

$$\left|\Psi_{1+n}^{Bell}\right\rangle = \left(\frac{1}{3}\left|00\right\rangle + e^{i2\pi n/3}\left|11\right\rangle + e^{-i2\pi n/3}\left|22\right\rangle\right), \tag{8.24}$$

$$\left|\Psi_{4+n}^{Bell}\right\rangle = \left(\frac{1}{3}\left|01\right\rangle + e^{i2\pi n/3}\left|12\right\rangle + e^{-i2\pi n/3}\left|20\right\rangle\right), \tag{8.25}$$

$$\left|\Psi_{7+n}^{Bell}\right\rangle = \left(\frac{1}{3}\left|02\right\rangle + e^{i2\pi n/3}\left|10\right\rangle + e^{-i2\pi n/3}\left|21\right\rangle\right). \tag{8.26}$$

where $n = 0, 1, 2$. All nine states lost their coherence completely under both collective and multi-local dephasing. However, first group of states, $\left|\Psi_1^{Bell}\right\rangle$, $\left|\Psi_2^{Bell}\right\rangle$, and $\left|\Psi_3^{Bell}\right\rangle$, are more fragile under dephasing since the interference terms of $\left|00\right\rangle$, and $\left|22\right\rangle$ decay with γ^{16}, and $\gamma_A^4\gamma_B^4$, for collective and multi-local dephasing, respectively. This type of classification of Bell-like states is in accordance with the previous study [137].

8.4 Horodecki's Bound Entangled State

Horodecki showed that following density matrix is bound entangled for $3 < a \leq 4$,

$$\rho(0) = \frac{2}{7}\mathbf{P}_+ + \frac{a}{7}\rho_+ + \frac{5-a}{7}\rho_-, \tag{8.27}$$

while it is separable for $2 \leq a \leq 3$ and free entangled for $4 < a \leq 5$ [42].

$$\mathbf{P}_+ = \frac{1}{3}\left(\left|00\right\rangle + \left|11\right\rangle + \left|22\right\rangle\right)\left(\left\langle00\right| + \left\langle11\right| + \left\langle22\right|\right), \tag{8.28}$$

$$\rho_+ = \frac{1}{3}\left(\left|01\right\rangle\left\langle01\right| + \left|12\right\rangle\left\langle12\right|\right) + \left|20\right\rangle\left\langle20\right|, \tag{8.29}$$

$$\rho_- = \frac{1}{3}\left(\left|10\right\rangle\left\langle10\right| + \left|21\right\rangle\left\langle21\right|\right) + \left|02\right\rangle\left\langle02\right|. \tag{8.30}$$

Time evolution of the density matrix becomes in the same form for both common and separate bath cases, such that

$$|\rho(t)| \approx \left[\frac{2}{21}\left(\left|00\right\rangle\left\langle00\right| + \left|11\right\rangle\left\langle11\right| + \left|22\right\rangle\left\langle22\right|\right)\right.$$

$$+ \left(\gamma\left|00\right\rangle\left\langle11\right| + H.c.\right) + \left(\gamma\left|22\right\rangle\left\langle11\right| + H.c.\right) + \left(\gamma^4\left|00\right\rangle\left\langle22\right| + H.c.\right)\right]$$

$$+ \frac{a}{7}\rho_+ + \frac{5-a}{7}\rho_-. \tag{8.31}$$

Here γ corresponds to γ_c, and $\gamma_{d,A}\gamma_{d,B}$ for common and different baths, respectively.

Negativity of this density matrix can be evaluated as

$$N = \max\{0, \frac{\|\rho^{T_A}\| - 1}{2}\}$$
$$= \frac{1}{42} \max\{\sqrt{(2a-5)^2 + 16|\gamma|^2} - 5\}. \tag{8.32}$$

Since $0 < \gamma \leq 1$, and $3 < a \leq 4$ for bound entangled state, negativity remains always zero. So, we use realignment criterion which can detect bound entangled states. Applying this criteria to our density matrix we get

$$R(\rho) = \frac{2}{21} \max\{0, \sqrt{3a^2 - 15a + 19} + 2(2\gamma + \gamma^4) - 7\}. \tag{8.33}$$

Critical value of the decoherence factor where bound entanglement complectly lost at $a = 4$ is equal to 0.84. Below this value two qutrit states become separable.

In order to compare the effect of common and separate baths, lets consider constant interaction strengths for both case, i.e. $\omega = \omega_k = \omega_{ki}$, then decoherence factors become

$$\gamma_c = e^{-8t^2\omega^2 \left(\sum_k^N |\alpha_k|^2 |\beta_k|^2 \right)} \tag{8.34}$$

$$\gamma_d = e^{-4t^2\omega^2 \left(\sum_k^{N_A} |\alpha_{kA}|^2 |\beta_{kA}|^2 + \sum_k^{N_B} |\alpha_{kB}|^2 |\beta_{kB}|^2 \right)}. \tag{8.35}$$

For large and random baths, terms in round parenthesis are approximately equal to each other assuming $N \approx N_A + N_B$. So, we see that first equation leads to more rapid decay. Then, bound entanglement of two qutrits is more robust to decoherence in multiple spin baths case than single spin bath case.

CHAPTER 9

Conclusion

We have studied the quantum tunneling of magnetization in $[\text{Mn}_4]_2$ dimer. Magnetization as a function of external longitudinal magnetic field is calculated using two approaches: exact time evolution solving the Schrodinger equation and the LZS theory. We found that these methods are consistent with each other. Hence, it is generally preferable to use LZS theory that requires much shorter computational time. We showed that magnetic field sweeping affects the tunneling transition rates. Also, we propose alternative spin states for the explanation of the observed steps in the hysteresis loops.

In the second part of our work, we introduced a decoherence model where the interaction between the central system and spin bath is mediated by phonons. We took the initial phonon states as a coherent state or thermal distribution. In the former case, decoherence factor decays in a Gaussian form and it becomes independent of the phonon frequencies Ω_k at short times $\Omega_k t \ll 1$. Also, the initial phonon states do not affect the decoherence factor if the phonon energies are much larger than spin-phonon coupling or bath spins are fully polarized. For the thermal distribution case, at low temperatures $T \ll \Omega_k$, short time decay of the decoherence factor is again in a Gaussian form and independent of the phonon frequencies. Phonons play a more important role in decoherence with increasing temperature. At high temperatures $T \gg \Omega_k$, decoherence factor becomes an exponentially decaying function of T. Later, we analyzed the effect of entangled environment on decoherence. We observed that entanglement within the environment reduces the decoherence of central spin. This result might be interpreted in terms of monogamous nature of entanglement. Finally, entanglement dynamics of the central bipartite spin system

is investigated. For common spin bath and separate spin bath cases, concurrences of the reduced density matrix of the central system have been calculated in terms of decoherence factors. In common spin bath, four Bell states are classified into a two group due to the presence of decoherence free subspace, while they lose their entanglement identically in the separate baths.

In the last part of the thesis, we examined the dephasing in entangled qutrits. We compared effects of the classical noise and quantum decoherence on the central pair of qutrits. We found equivalent results for both cases at the level of density matrix formalism. For common and separate baths, we determine the robust and fragile Bell-like qutrit states. Horodecki's bound entangled state is shown to be more robust to decoherence in the latter case.

Appendix A

Time Evolution of Bath for Coherent Phonon States

In this Appendix, we give the details of the calculations in derivation of the time-dependent bath state $|B_\pm(t)\rangle$ in Eq. (7.4). Note that Hamiltonian in Eq. (7.1) can be written as

$$H = \sum_{k=1}^{N} H_k, \tag{A.1}$$

where

$$H_k = c_z \left[\omega_{0k} + \omega_k(p_k^\dagger + p_k) \right] s_{kz} + \Omega_k p_k^\dagger p_k. \tag{A.2}$$

Noting that all the terms commute with each other $[H_k, H_{k'}] = \delta_{k,k'}$, time evolution operator can be expressed in the following form

$$U(t) = e^{-itH} = e^{-it\sum_k^N H_k} = \prod_{k=1}^{N} e^{-itH_k}. \tag{A.3}$$

Since we take initial states in product form as in Eq. (7.2), time evolution of the total system can be easily derived once we calculate the terms

$$e^{-itH_k}|m_c\rangle|n_k\rangle|\lambda_k\rangle, \tag{A.4}$$

where the states are written in the order of central spin, bath spin, and phonon mode. Here m_c and n_k take the values -1 and 1 corresponding to spin-up state and spin-down state, respectively. Since H_k commutes with Pauli spin operators of central system c_z and bath spin s_{kz}, only effect of the above time evolution operator is on the phonon state $|\lambda_k\rangle$. The states $|m_c\rangle$ and $|n_k\rangle$ remain unchanged during time

evolution

$$e^{-itH_k}|m_c\rangle|n_k\rangle|\lambda_k\rangle = |m_c\rangle|n_k\rangle e^{-itH_k^{m_c,n_k}}|\lambda_k\rangle. \tag{A.5}$$

Here $H_k^{m_c,n_k} = m_c n_k[\omega_{0k} + \omega_k(p_k^\dagger + p_k)] + \Omega_k p_k^\dagger p_k$. Thus, signs of the coupling constants ω_{0k} and ω_k depend on the relative orientations of the central spin and bath spin. Let us calculate the case where they are parallel to each other and label the corresponding Hamiltonian as $H_{k+} = \omega_{0k} + \omega_k(p_k^\dagger + p_k) + \Omega_k p_k^\dagger p_k$. After this point we omit the label k for simpler notation.

We first note that it is possible to write H_+ in diagonal form with respect to phonon number operator $p^\dagger p$ by applying the following transformation

$$H_+' = D\left(\frac{\omega}{\Omega}\right)H_+D^\dagger\left(\frac{\omega}{\Omega}\right) = \Omega p^\dagger p - \frac{\omega^2}{\Omega} + \omega_0, \tag{A.6}$$

where $D(\alpha) = e^{\alpha p^\dagger + \alpha^* p}$ is called as displacement operator. This operator is unitary $D^\dagger(\alpha)D(\alpha) = \mathbf{1}$ and it displaces the annihilation and creation operators: $D^\dagger(\alpha)pD(\alpha) = p + \alpha$, $D^\dagger(\alpha)p^\dagger D(\alpha) = p^\dagger + \alpha^*$. Also, it creates a coherent state by acting on a vacuum state $D(\alpha)|0\rangle = |\alpha\rangle$.

Now we are ready to evaluate the time evolution of the coherent phonon states $|\lambda\rangle$ under Hamiltonian H_+. Introducing $\xi = \frac{\omega}{\Omega}$, we calculate the following

$$\begin{aligned} e^{-itH_+}|\lambda\rangle &= D^\dagger(\xi)D(\xi)e^{-itH}D^\dagger(\xi)D(\xi)|\lambda\rangle \\ &= D^\dagger(\xi)e^{-itH_+'}D(\xi)|\lambda\rangle \\ &= D^\dagger(\xi)e^{-itH_+'}D(\xi)D(\lambda)|0\rangle \\ &= D^\dagger(\xi)e^{-itH_+'}e^{\frac{\xi}{2}(\lambda^*-\lambda)}|\xi + \lambda\rangle, \end{aligned} \tag{A.7}$$

where at the last step we use the following property of displacement operator: $D(\alpha)D(\beta) = e^{(\alpha\beta^*-\alpha^*\beta)/2}D(\alpha+\beta)$. Continuing the above calculation, we find

$$\begin{aligned} e^{-itH_+}|\lambda\rangle &= e^{\frac{\xi}{2}(\lambda^*-\lambda)}D^\dagger(\xi)e^{-it\left[\omega_0+\omega(p^\dagger+p)+\Omega p^\dagger p\right]}|\xi + \lambda\rangle \\ &= e^{\frac{\xi}{2}(\lambda^*-\lambda)}e^{-it(\omega_0-\xi^2\Omega)}D^\dagger(\xi)|(\xi+\lambda)e^{-it\Omega}\rangle \\ &= e^{\frac{\xi}{2}(\lambda^*-\lambda)}e^{-it(\omega_0-\xi^2\Omega)}e^{\frac{\xi}{2}\left[(\xi+\lambda)e^{-it\Omega}-(\xi+\lambda^*)e^{it\Omega}\right]}|(\xi+\lambda)e^{-it\Omega}-\xi\rangle. \end{aligned} \tag{A.8}$$

Now if we reorganize the final result in terms of imaginary and real parts of the λ, we find that it is equal to A_k^+ in Eq. (7.6) (reintroducing the labels k)

$$\begin{aligned} e^{-itH_+}|\lambda_k\rangle = A_k^+|\lambda_k\rangle &= e^{i\frac{\omega_k^2}{\Omega_k}\left(t-\frac{\sin(\Omega_k t)}{\Omega_k}\right)}e^{-it\omega_{0k}} \\ &\times e^{-i\frac{\omega_k}{\Omega_k}[\mathrm{Re}[\lambda_k]\sin(\Omega_k t)+\mathrm{Im}[\lambda_k](1-\cos(\Omega_k t))]}|\lambda_k\rangle. \end{aligned} \tag{A.9}$$

When the central spin and bath spin are anti-parallel to each other, time evolution of the coherent state is governed by the Hamiltonian $H_{k-} = -\omega_{0k} - \omega_k(p_k^\dagger + p_k) + \Omega_k p_k^\dagger p_k$. Only difference from the previous result will be the sign changes in coupling parameters ω_{0k} and ω_k such that $e^{-itH_-}|\lambda_k\rangle = A_k^-|\lambda_k\rangle$. Then, it is straight forward to obtain the time dependent wavefunction of the bath $|B_\pm(t)\rangle$ in Eq. (7.4).

Appendix B

Decoherence Factor for Thermal Distribution

Here we give the detailed calculation of the decoherence factor in Eq. (7.16) that is obtained for thermal phonon states. Density matrix of the phonons in thermal distribution is given by

$$\rho_p(0) = \bigotimes_k^N \rho_{p,k}(0)$$

$$= \bigotimes_k^N (1 - e^{-\frac{\Omega_k}{T}}) \sum_{n_k=0}^{\infty} e^{-\frac{\Omega_k n_k}{T}} |n_k\rangle\langle n_k|. \tag{B.1}$$

We assume the same product form for the bath spins

$$\rho_s(0) = [\bigotimes_k^N (\alpha_k|\uparrow_k\rangle + \beta_k|\downarrow_k\rangle)][\text{c. c.}]. \tag{B.2}$$

Time evolution of the total density matrix can be evaluated as

$$\rho(t) = e^{-itH}\rho_c(0)\rho_s(0)\rho_p(0)e^{itH}. \tag{B.3}$$

Upper off-diagonal element of the central system's reduced density matrix $\rho_c^{\daleth}$ can be calculated by taking the trace over bath spins and phonons such that

$$\rho_c^{\daleth}(t) = c_\uparrow c_\downarrow^*|\uparrow\rangle\langle\downarrow|r(t) = Tr_{bath}\left[e^{-itH}c_\uparrow c_\downarrow^*|\uparrow\rangle\langle\downarrow|\rho_s(0)\rho_p(0)e^{itH}\right], \tag{B.4}$$

where $r(t)$ is decoherence factor, and $H_\pm$ is introduced in previous Appendix. It can be easily shown by the help of previous Appendix that $\rho_c^{\daleth}$ is given as the following

$$\rho_c^{\daleth}(t) = c_\uparrow c_\downarrow^*|\uparrow\rangle\langle\downarrow|\prod_k^N Tr_p\left[|\alpha_k|^2 e^{-itH_k^+}\rho_{p,k}(0)e^{itH_k^-} + |\beta_k|^2 e^{-itH_k^-}\rho_{p,k}(0)e^{itH_k^+}\right]. \tag{B.5}$$

Let us first calculate the term $(e^{-itH_k^+}\rho_{p,k}(0)e^{itH_k^-})$ which we simply denote as ρ_p'. Again, we omit the labels k for clearer notation. We insert the over-completeness relation of coherent states

$$\mathbf{1} = \frac{1}{\pi}\int d^2\gamma|\gamma\rangle\langle\gamma| \tag{B.6}$$

into the ρ_p' expression such that

$$\rho_p' = (1 - e^{-\frac{\Omega}{T}})\frac{1}{\pi}\int d^2\gamma(e^{-itH^+}|\gamma\rangle)\sum_n e^{-\frac{\omega n}{T}}(\langle\gamma|n\rangle)\langle n|e^{itH^-}$$

$$= (1 - e^{-\frac{\Omega}{T}})\frac{1}{\pi}\int d^2\gamma(A_\gamma^+|u_\gamma^+\rangle)\sum_n e^{-\frac{\omega n}{T}}(e^{-\frac{|\gamma|^2}{2}}\frac{\gamma^{*n}}{\sqrt{n!}})\langle n|e^{itH^-}, \tag{B.7}$$

where $A_\gamma^\pm$ and $u_\gamma^\pm$ are the same expression as previously introduced in Eq. (7.6) and Eq. (7.5), respectively, except λ is replaced by γ. Inserting another identity operator inside the ρ_p' expression, we find

$$\rho_p' = (1 - e^{-\frac{\Omega}{T}})\frac{1}{\pi^2}\iint d^2\gamma d^2\zeta(A_\gamma^+|u_\gamma^+\rangle)\sum_n e^{-\frac{\omega n}{T}}(e^{-\frac{|\gamma|^2}{2}}\frac{\gamma^{*n}}{\sqrt{n!}})(\langle n|\zeta\rangle)(\langle\zeta|e^{itH^-})$$

$$= (1 - e^{-\frac{\Omega}{T}})\frac{1}{\pi^2}\iint d^2\gamma d^2\zeta(A_\gamma^+|u_\gamma^+\rangle)\sum_n e^{-\frac{\omega n}{T}}(e^{-\frac{|\gamma|^2}{2}}\frac{\gamma^{*n}}{\sqrt{n!}})(e^{-\frac{|\zeta|^2}{2}}\frac{\zeta^n}{\sqrt{n!}})(\langle u_\zeta^-|A_\zeta^{-*})$$

$$= (1 - e^{-\frac{\Omega}{T}})\frac{1}{\pi^2}\iint d^2\gamma d^2\zeta A_\gamma^+ A_\zeta^{-*}|u_\gamma^+\rangle\langle u_\zeta^-|e^{-\frac{|\gamma|^2+|\zeta|^2}{2}}e^{-\frac{\omega}{T}\gamma^*\zeta}. \tag{B.8}$$

Now we take the trace of this expression over phonon coherent states such that

$$Tr_p\rho_p' = \frac{1}{\pi}\int d^2\chi\langle\chi|\rho_p'|\chi\rangle$$

$$= (1 - e^{-\frac{\Omega}{T}})\frac{1}{\pi^3}\iiint d^2\gamma d^2\zeta d^2\chi A_\gamma^+ A_\zeta^{-*}e^{-\frac{|\gamma|^2+|\zeta|^2}{2}}e^{-\frac{\omega}{T}\gamma^*\zeta}\langle\chi|u_\gamma^+\rangle\langle u_\zeta^-|\chi\rangle$$

$$= (1 - e^{-\frac{\Omega}{T}})\frac{1}{\pi^3}\iiint d^2\gamma d^2\zeta d^2\chi A_\gamma^+ A_\zeta^{-*}e^{-\frac{|\gamma|^2+|\zeta|^2}{2}}e^{-\frac{\omega}{T}\gamma^*\zeta}$$

$$\times(e^{-\frac{|\chi|^2}{2}}e^{-\frac{|u_\gamma^+|^2}{2}}e^{\chi^* u_\gamma^+})(e^{-\frac{|\chi|^2}{2}}e^{-\frac{|u_\zeta^-|^2}{2}}e^{u_\zeta^{-*}\chi})$$

$$= (1 - e^{-\frac{\Omega}{T}})\frac{1}{\pi^3}\iint d^2\gamma d^2\zeta A_\gamma^+ A_\zeta^{-*}e^{-\frac{|\gamma|^2+|\zeta|^2+|u_\gamma^+|^2+|u_\zeta^-|^2}{2}}e^{-\frac{\omega}{T}\gamma^*\zeta}\int d^2\chi F(\chi), \tag{B.9}$$

where $F(\chi) = e^{-|\chi|^2}e^{\chi^* u_\gamma^+}e^{u_\zeta^{-*}\chi}$. The last integral $\int d^2\chi F(\chi)$ is equal to $\pi e^{u_\zeta^{-*}u_\gamma^+}$. Later two integrals will also have similar structure to this integral. More general formula for this kind of integrals is $\int d^2z e^{-\alpha|z|^2+\alpha z'z^*}f(z) = \frac{\pi}{d}f(z')$. Then, the above

calculation follows as

$$
\begin{aligned}
Tr_p\rho'_p &= (1-e^{-\frac{\Omega}{T}})\frac{1}{\pi^2}\int d^2\gamma A_\gamma^+ e^{-\frac{|\gamma|^2+|u_\gamma^+|^2}{2}}\int d^2\zeta A_\zeta^{-*}e^{-\frac{|\zeta|^2+|u_\zeta^{-*}|^2}{2}}e^{e^{-\frac{\omega}{T}}\gamma^*\zeta}e^{u_\zeta^{-*}u_\gamma^+}\\
&= (1-e^{-\frac{\Omega}{T}})\frac{1}{\pi^2}\int d^2\gamma A_\gamma^+ e^{-\frac{|\gamma|^2+|u_\gamma^+|^2}{2}}\\
&\quad \times \pi e^{-i\frac{\omega^2}{\Omega}(t-\frac{\sin(\Omega t)}{\Omega})-it\omega_0}e^{-\frac{\omega^2}{\Omega^2}(1-\cos(\Omega t))}e^{\frac{\omega}{\Omega}(1-e^{it\Omega})u_\gamma^+}e^{\gamma^* e^{-\frac{\Omega}{T}}[\frac{\omega}{\Omega}(1-e^{it\Omega})+e^{it\Omega}u_\gamma^+]}\\
&= (1-e^{-\frac{\Omega}{T}})\frac{1}{\pi}e^{-2it\omega_0}e^{-4\frac{\omega^2}{\Omega^2}(1-\cos(\Omega t))}\\
&\quad \times \int d^2\gamma e^{-|\gamma|^2(1-e^{-\frac{\Omega}{T}})}e^{-\frac{2\omega}{\Omega}(1-e^{-it\Omega})\gamma}e^{\frac{2\omega}{\Omega}e^{-\frac{\Omega}{T}}(1-e^{it\Omega})\gamma^*}\\
&= (1-e^{-\frac{\Omega}{T}})\frac{1}{\pi}e^{-2it\omega_0}e^{-4\frac{\omega^2}{\Omega^2}(1-\cos(\Omega t))}\left(\frac{\pi}{1-e^{-\frac{\Omega}{T}}}e^{-8\frac{\omega^2}{\Omega^2}(1-\cos(\Omega t))\frac{e^{-\frac{\Omega}{T}}}{1-e^{-\frac{\Omega}{T}}}}\right)\\
&= e^{-2it\omega_0}e^{-4\frac{\omega^2}{\Omega^2}(1-\cos(\Omega t))\coth(\frac{\Omega}{2T})}.
\end{aligned}
\tag{B.10}
$$

Then, $\rho_c^{\neg}$ is given as

$$
\rho_c^{\neg}(t) = c_\uparrow c_\downarrow^* |\uparrow\rangle\langle\downarrow|\prod_k^N e^{-4\frac{\omega^2}{\Omega^2}(1-\cos(\Omega t))\coth(\frac{\Omega}{2T})}(|\alpha|^2 e^{-2it\omega_0}+|\beta|^2 e^{2it\omega_0}).
\tag{B.11}
$$

Bibliography

[1] Bohr, N. (1928). The quantum postulate and the recent development of atomic theory. Nature, 121(3050), 580.

[2] Zurek, W. H. (1981). Pointer basis of quantum apparatus: Into what mixture does the wave packet collapse? Physical Review D, 24(6), 1516.

[3] Zurek, W. H. (1982). Environment-induced superselection rules. Physical Review D, 26(8), 1862.

[4] Einstein, A., Podolsky, B., and Rosen, N. (1935). Can quantum-mechanical description of physical reality be considered complete? Physical Review, 47(10), 777.

[5] Bell, J. S. (1964). On the Einstein-Podolsky-Rosen paradox. Physics , 1, 195.

[6] Freedman, S. J., and Clauser, J. F. (1972). Experimental test of local hidden-variable theories. Physical Review Letters, 28(14), 938.

[7] Aspect, A., Grangier, P., and Roger, G. (1981). Experimental tests of realistic local theories via Bell's theorem. Physical Review Letters, 47(7), 460.

[8] Aspect, A., Grangier, P., and Roger, G. (1982). Experimental realization of Einstein-Podolsky-Rosen-Bohm gedankenexperiment: A new violation of Bell's inequalities. Physical Review Letters, 49(2), 91.

[9] Aspect, A., Dalibard, J., and Roger, G. (1982). Experimental test of Bell's inequalities using time-varying analyzers. Physical Review Letters, 49(25), 1804.

[10] Weihs, G., Jennewein, T., Simon, C., Weinfurter, H., and Zeilinger, A. (1998). Violation of Bell's inequality under strict Einstein locality conditions. Physical Review Letters, 81(23), 5039.

[11] Nielsen, M. A., and Chuang, I. L. (2000). Quantum computation and quantum information. Cambridge University Press.

[12] Shor, P. W. (1994). Algorithms for quantum computation: Discrete logarithms and factoring. Proceedings of the 35th Annual Symposium on Foundations of Computer Science, 124.

[13] Loss, D., and DiVincenzo, D. P. (1998). Quantum computation with quantum dots. Physical Review A, 57(1), 120.

[14] Gatteschi, D., and Sessoli, R. (2003). Quantum tunneling of magnetization and related phenomena in molecular materials. Angewandte Chemie International Edition, 42(3), 268.

[15] Ardavan, A., Rival, O., Morton, J. J. L., Blundell, S. J., Tyryshkin, A. M., Timco, G. A., et al. (2007). Will spin-relaxation times in molecular magnets permit quantum information processing? Physical Review Letters, 98(5), 57201.

[16] Bertaina, S., Gambarelli, S., Mitra, T., Tsukerblat, B., Muller, A., and Barbara, B. (2008). Quantum oscillations in a molecular magnet. Nature, 453(7192), 203.

[17] Friedman, J. R., Sarachik, M. P., Tejada, J., and Ziolo, R. (1996). Macroscopic measurement of resonant magnetization tunneling in high-spin molecules. Physical Review Letters, 76(20), 3830.

[18] Thomas, L., Lionti, F., Ballou, R., Gatteschi, D., Sessoli, R., and Barbara, B. (1996). Macroscopic quantum tunnelling of magnetization in a single crystal of nanomagnets. Nature, 383(6596), 145.

[19] Wernsdorfer, W., Aliaga-Alcalde, N., Hendrickson, D. N., and Christou, G. (2002). Exchange-biased quantum tunnelling in a supramolecular dimer of single-molecule magnets. Nature, 416(6879), 406.

[20] Bagai, R., Wernsdorfer, W., Abboud, K. A., and Christou, G. (2007). Exchange-biased dimers of single-molecule magnets in off and on states. Journal of the American Chemical Society, 129(43), 12918.

[21] Ramsey, C., Del Barco, E., Hill, S., Shah, S., Beedle, C., and Hendrickson, D. (2008). Quantum interference of tunnel trajectories between states of different spin length in a dimeric molecular nanomagnet. Nature Physics, 4(4), 277.

[22] Chen, J. L., Kaszlikowski, D., Kwek, L. C., Oh, C. H., and Zukowski, M. (2001). Entangled three-state systems violate local realism more strongly than qubits: An analytical proof. Physical Review A, 64(5), 52109.

[23] Kaszlikowski, D., Gnacinski, P., Zukowski, M., Miklaszewski, W., and Zeilinger, A. (2000). Violations of local realism by two entangled n-dimensional systems are stronger than for two qubits. Physical Review Letters, 85(21), 4418.

[24] Collins, D., Gisin, N., Linden, N., Massar, S., and Popescu, S. (2002). Bell inequalities for arbitrarily high-dimensional systems. Physical Review Letters, 88(4), 040404.

[25] Bechmann-Pasquinucci, H., and Peres, A. (2000). Quantum cryptography with 3-state systems. Physical Review Letters, 85(15), 3313.

[26] Bourennane, M., Karlsson, A., and Björk, G. (2001). Quantum key distribution using multilevel encoding. Physical Review A, 64(1), 012306.

[27] Spekkens, R. W., and Rudolph, T. (2001). Degrees of concealment and bindingness in quantum bit commitment protocols. Physical Review A, 65(1), 012310.

[28] Cerf, N. J., Bourennane, M., Karlsson, A., and Gisin, N. (2002). Security of quantum key distribution using d-level systems. Physical Review Letters, 88(12), 127902.

[29] Bruß, D., and Macchiavello, C. (2002). Optimal eavesdropping in cryptography with three-dimensional quantum states. Physical Review Letters, 88(12), 127901.

[30] Durt, T., Cerf, N. J., Gisin, N., and Z.ukowski, M. (2003). Security of quantum key distribution with entangled qutrits. Physical Review A, 67(1), 012311.

[31] Langford, N. K., Dalton, R. B., Harvey, M. D., O'Brien, J. L., Pryde, G. J., Gilchrist, A., et al. (2004). Measuring entangled qutrits and their use for quantum bit commitment. Physical Review Letters, 93(5), 053601.

[32] Gröblacher, S., Jennewein, T., Vaziri, A., Weihs, G., and Zeilinger, A. (2006). Experimental quantum cryptography with qutrits. New Journal of Physics, 8, 75.

[33] Ralph, T. C., Resch, K. J., and Gilchrist, A. (2007). Efficient Toffoli gates using qudits. Physical Review A, 75(2), 022313.

[34] Shor, P. W. (1995). Scheme for reducing decoherence in quantum computer memory. Physical Review A, 52(4), 2493.

[35] Lidar, D. A., Chuang, I. L., and Whaley, K. B. (1998). Decoherence-free subspaces for quantum computation. Physical Review Letters, 81(12), 2594.

[36] Tonomura, A., Endo, J., Matsuda, T., Kawasaki, T., and Ezawa, H. (1989). Demonstration of single-electron build-up of an interference pattern. American Journal of Physics, 57(2), 117.

[37] Werner, R. F. (1989). Quantum states with Einstein-Podolsky-Rosen correlations admitting a hidden-variable model. Physical Review A, 40(8), 4277.

[38] Shi, Y. (2003). Quantum entanglement of identical particles. Physical Review A, 67(2), 024301.

[39] Schmidt, E. (1907). Zur Theorie der linearen und nichtlinearen Integralgleichungen. Mathematische Annalen, 63(4), 433.

[40] Peres, A. (1996). Separability criterion for density matrices. Physical Review Letters, 77(8), 1413.

[41] Horodecki, M., Horodecki, P., and Horodecki, R. (1996). Separability of mixed states: necessary and sufficient conditions. Physics Letters A, 223(1-2), 1.

[42] Horodecki, M., Horodecki, P., and Horodecki, R. (1998). Mixed-state entanglement and distillation: Is there a "bound" entanglement in nature? Physical Review Letters, 80(24), 5239.

[43] Dür, W., Cirac, J. I., Lewenstein, M., and Bruß, D. (2000). Distillability and partial transposition in bipartite systems. Physical Review A, 61(6), 62313.

[44] DiVincenzo, D. P., Shor, P. W., Smolin, J. A., Terhal, B. M., and Thapliyal, A. V. (2000). Evidence for bound entangled states with negative partial transpose. Physical Review A, 61(6), 62312.

[45] Kraus, B., Lewenstein, M., and Cirac, J. I. (2002). Characterization of distillable and activatable states using entanglement witnesses. Physical Review A, 65(4), 042327.

[46] Horodecki, P., Horodecki, M., and Horodecki, R. (1999). Bound entanglement can be activated. Physical Review Letters, 82(5), 1056.

[47] Horodecki, K., Horodecki, M., Horodecki, P., and Oppenheim, J. (2005). Secure key from bound entanglement. Physical Review Letters, 94(16), 160502.

[48] Horodecki, P., and Augusiak, R. (2006). On quantum cryptography with bipartite bound entangled states. Quantum information processing: From theory to experiment,(Edited by D.G. Angelakis et al.), NATO Science Series, 199, 19. IOS Press, Amsterdam.

[49] Chen, K., and Wu, L. A. (2003). A matrix realignment method for recognizing entanglement. Quantum Information and Computation, 3(3), 193.

[50] Rudolph, O. (2005). Further results on the cross norm criterion for separability. Quantum Information Processing, 4(3), 219.

[51] Terhal, B. M. (2002). Detecting quantum entanglement. Theoretical Computer Science, 287(1), 313.

[52] Plenio, M. B., and Virmani, S. (2007). An introduction to entanglement measures. Quantum Information and Computation, 7(1-2), 1.

[53] Mintert, F., Carvalho, A. R. R., Kus, M., and Buchleitner, A. (2005). Measures and dynamics of entangled states. Physics Reports, 415(4), 207.

[54] Bennett, C. H., DiVincenzo, D. P., Smolin, J. A., and Wootters, W. K. (1996). Mixed-state entanglement and quantum error correction. Physical Review A, 54(5), 3824.

[55] Bennett, C. H., Bernstein, H. J., Popescu, S., and Schumacher, B. (1996). Concentrating partial entanglement by local operations. Physical Review A, 53(4), 2046.

[56] Cohen, O. (1998). Unlocking hidden entanglement with classical information. Physical Review Letters, 80(11), 2493.

[57] Von Neumann, J. (1932). Mathematische grundlagen der quantenmechanik. Springer, Berlin.

[58] Von Neumann, J. (1955). Mathematical foundations of quantum mechanics. Princeton University Press, Princeton.

[59] Wootters, W. K. (1998). Entanglement of formation of an arbitrary state of two qubits. Physical Review Letters, 80(10), 2245.

[60] Vidal, G., and Werner, R. F. (2002). Computable measure of entanglement. Physical Review A, 65(3), 32314.

[61] Christandl, M., and Winter, A. (2004). "Squashed entanglement": An additive entanglement measure. Journal of Mathematical Physics, 45(3), 829.

[62] Rényi, A. (1970). Probability theory. Dover Publications, Amsterdam.

[63] Vedral, V., Plenio, M. B., Rippin, M. A., and Knight, P. L. (1997). Quantifying entanglement. Physical Review Letters, 78(12), 2275.

[64] Audenaert, K., Plenio, M. B., and Eisert, J. (2003). Entanglement cost under positive-partial-transpose-preserving operations. Physical Review Letters, 90(2), 27901.

[65] Rains, E. M. (1999). Bound on distillable entanglement. Physical Review A, 60(1), 179.

[66] Verstraete, F., Audenaert, K., Dehaene, J., and DeMoor, B. (2001). A comparison of the entanglement measures negativity and concurrence. Journal of Physics A: Mathematical and General, 34(47), 10327.

[67] Zurek, W. H. (2003). Decoherence, einselection, and the quantum origins of the classical. Reviews of Modern Physics, 75(3), 715.

[68] Schlosshauer, M. (2005). Decoherence, the measurement problem, and interpretations of quantum mechanics. Reviews of Modern Physics, 76(4), 1267.

[69] Cucchietti, F. M., Pastawski, H. M., and Wisniacki, D. A. (2002). Decoherence as decay of the Loschmidt echo in a Lorentz gas. Physical Review E, 65(4), 45206.

[70] Cucchietti, F. M., Dalvit, D. A. R., Paz, J. P., and Zurek, W. H. (2003). Decoherence and the Loschmidt echo. Physical Review Letters, 91(21), 210403.

[71] Cucchietti, F. M., Paz, J. P., and Zurek, W. H. (2005). Decoherence from spin environments. Physical Review A, 72(5), 52113.

[72] Prokof'ev, N. V., and Stamp, P. C. E. (1996). Quantum relaxation of magnetisation in magnetic particles. Journal of Low Temperature Physics, 104(3), 143.

[73] Prokof'ev, N. V., and Stamp, P. C. E. (1998). Low-temperature quantum relaxation in a system of magnetic nanomolecules. Physical Review Letters, 80(26), 5794.

[74] Prokof'ev, N. V., and Stamp, P. C. E. (2000). Theory of the spin bath. Reports on Progress in Physics, 63(4), 669.

[75] Feynman, R. P., and Vernon, F. L. (1963). The theory of a general quantum system interacting with a linear dissipative system. Annals of Physics, 24, 118.

[76] Caldeira, A. O., and Leggett, A. J. (1981). Influence of dissipation on quantum tunneling in macroscopic systems. Physical Review Letters, 46(4), 211.

[77] Caldeira, A. O., and Leggett, A. J. (1983). Dissipation and quantum tunnelling. Annals of Physics, 149(2), 374.

[78] Leggett, A. J., Chakravarty, S., Dorsey, A. T., Fisher, M. P. A., Garg, A., and Zwerger, W. (1987). Dynamics of the dissipative two-state system. Reviews of Modern Physics, 59(1), 1.

[79] Weiss, U. (1999). Quantum dissipative systems. Series in Modern Condensed Matter Physics Vol. 10, World Scientific Pub Co Inc, Singapore.

[80] Lounasmaa, O. V. (1974). Experimental principles and methods below 1 K. Academic Press, New York.

[81] Khaetskii, A. V., Loss, D., and Glazman, L. (2002). Electron spin decoherence in quantum dots due to interaction with nuclei. Physical Review Letters, 88(18), 186802.

[82] Merkulov, I. A., Efros, A. L., and Rosen, M. (2002). Electron spin relaxation by nuclei in semiconductor quantum dots. Physical Review B, 65(20), 205309.

[83] Schliemann, J., Khaetskii, A. V., and Loss, D. (2002). Spin decay and quantum parallelism. Physical Review B, 66(24), 245303.

[84] Tessieri, L., and Wilkie, J. (2003). Decoherence in a spin spin-bath model with environmental self-interaction. Journal of Physics A: Mathematical and General, 36(49), 12305.

[85] Dobrovitski, V. V., and De Raedt, H. A. (2003). Efficient scheme for numerical simulations of the spin-bath decoherence. Physical Review E, 67(5), 56702.

[86] Coish, W. A., and Loss, D. (2004). Hyperfine interaction in a quantum dot: Non-Markovian electron spin dynamics. Physical Review B, 70(19), 195340.

[87] Deng, C., and Hu, X. (2006). Analytical solution of electron spin decoherence through hyperfine interaction in a quantum dot. Physical Review B, 73(24), 241303.

[88] Gedik, Z., and Bozat, Ö. (2006). Quantum tunnelling and decoherence in nanomagnets. Physica Status Solidi C 3(5), 1268.

[89] Camalet, S., and Chitra, R. (2007). Effect of random interactions in spin baths on decoherence. Physical Review B, 75(9), 094434.

[90] Zhang, W. X., Konstantinidis, N., Al-Hassanieh, K. A., and Dobrovitski, V. V. (2007). Modelling decoherence in quantum spin systems . Journal of Physics: Condensed Matter, 19(19), 1.

[91] Troiani, F., Bellini, V., and Affronte, M. (2008). Decoherence induced by hyperfine interactions with nuclear spins in antiferromagnetic molecular rings. Physical Review B, 77(5), 54428.

[92] Gatteschi, D., Caneschi, A., Pardi, L., and Sessoli, R. (1994). Large clusters of metal ions: The transition from molecular to bulk magnets. Science, 265(5175), 1054.

[93] Sessoli, R., Gatteschi, D., Caneschi, A., and Novak, M. A. (1993). Magnetic bistability in a metal-ion cluster. Nature, 365(6442), 141.

[94] Cornia, A., Fabretti, A. C., Pacchioni, M., Zobbi, L., Bonacchi, D., Caneschi, A., et al. (2003). Direct observation of single-molecule magnets organized on gold surfaces. Angewandte Chemie International Edition, 42(14), 1645.

[95] Heersche, H. B., de Groot, Z., Folk, J. A., van der Zant, H. S. J., Romeike, C., Wegewijs, M. R., et al. (2006). Electron transport through single Mn_{12} molecular magnets. Physical Review Letters, 96(20), 206801.

[96] Jo, M., Grose, J., Baheti, K., Deshmukh, M., Sokol, J., Rumberger, E., et al. (2006). Signatures of molecular magnetism in single-molecule transport spectroscopy. Nano Letters, 6(9), 2014.

[97] Wernsdorfer, W., and Sessoli, R. (1999). Quantum phase interference and parity effects in magnetic molecular clusters. Science, 284(5411), 133.

[98] Meier, F., Levy, J., and Loss, D. (2003). Quantum computing with spin cluster qubits. Physical Review Letters, 90(4), 47901.

[99] Affronte, M., Troiani, F., Ghirri, A., Candini, A., Evangelisti, M., Corradini, V., et al. (2007). Single molecule magnets for quantum computation. Journal of Physics D, Applied Physics, 40(10), 2999.

[100] Leunberger, M., and Loss, D. (2001). Quantum computing in molecular magnets. Nature, 410(6830), 789.

[101] Caneschi, A., Gatteschi, D., Sangregorio, C., Sessoli, R., Sorace, L., Cornia, A., et al. (1999). The molecular approach to nanoscale magnetism. Journal of magnetism and magnetic materials, 200(1-3), 182.

[102] Landau, L. D. (1932). Zur theorie der energieubertragung bei stoen. Phys. Z. Sowjetunion, 2, 46.

[103] Zener, C. (1932). Non-adiabatic crossing of energy levels. Proceedings of the Royal Society of London. Series A, Containing Papers of a Mathematical and Physical Character (1905-1934), 137(833), 696.

[104] Stückelberg, E. C. G. (1932). Theory of inelastic collisions between atoms. Helvetica Physical Acta, 5, 369.

[105] Stamp, P. C. E., and Tupitsyn, I. S. (2004). Coherence window in the dynamics of quantum nanomagnets. Physical Review B, 69(1), 14401.

[106] Wernsdorfer, W., Chakov, N. E., and Christou, G. (2005). Quantum phase interference and spin-parity in Mn_{12} single-molecule magnets. Physical Review Letters, 95(3), 037203.

[107] Evangelisti, M., Luis, F., Mettes, F. L., Aliaga, N., Arom, G., Alonso, J. J., et al. (2004). Magnetic long-range order induced by quantum relaxation in single-molecule magnets. Physical Review Letters, 93(11), 117202.

[108] Morello, A., Bakharev, O. N., Brom, H. B., Sessoli, R., and de Jongh, L. J. (2004). Nuclear spin dynamics in the quantum regime of a single-molecule magnet. Physical Review Letters, 93(19), 197202.

[109] Evangelisti, M., Luis, F., Mettes, F. L., Sessoli, R., and de Jongh, L. J. (2005). Giant isotope effect in the incoherent tunneling specific heat of the molecular nanomagnet Fe_8. Physical Review Letters, 95(22), 227206.

[110] Morello, A., and de Jongh, L. J. (2007). Dynamics and thermalization of the nuclear spin bath in the single-molecule magnet Mn_{12}-ac: Test for the theory of spin tunneling. Physical Review B, 76(18), 184425.

[111] Waller, I. (1932). ber die magnetisierung von paramagnetischen kristallen in wechselfeldern. Zeitschrift fr Physik A Hadrons and Nuclei, 79(5), 370.

[112] Abalmassov, V. A., and Marquardt, F. (2004). Electron-nuclei spin relaxation through phonon-assisted hyperfine interaction in a quantum dot. Physical Review B, 70(7), 75313.

[113] Jaksch, D., Briegel, H., Cirac, J. I., Gardiner, C. W., and Zoller, P. (1999). Entanglement of atoms via cold controlled collisions. Physical Review Letters, 82(9), 1975.

[114] Aubin, S., Wemple, M., Adams, D., Tsai, H., Christou, G., and Hendrickson, D. (1996). Distorted $Mn^{IV}Mn_3^{III}$ cubane complexes as single-molecule magnets. Journal of the American Chemical Society, 118(33), 7746.

[115] Aubin, S. M. J., Dilley, N. R., Wemple, M. W., Maple, M. B., Christou, G., and Hendrickson, D. N. (1998). Half-integer-spin small molecule magnet exhibiting resonant magnetization tunneling. Journal of the American Chemical Society, 120(4), 839.

[116] Wernsdorfer, W., Bhaduri, S., Boskovic, C., Christou, G., and Hendrickson, D. N. (2002). Spin-parity dependent tunneling of magnetization in single-molecule magnets. Physical Review B, 65(18), 180403.

[117] Hill, S., Edwards, R. S., Aliaga-Alcalde, N., and Christou, G. (2003). Quantum coherence in an exchange-coupled dimer of single-molecule magnets. Science, 302(5647), 1015.

[118] Tiron, R., Wernsdorfer, W., Foguet-Albiol, D., Aliaga-Alcalde, N., and Christou, G. (2003). Spin quantum tunneling via entangled states in a dimer of exchange-coupled single-molecule magnets. Physical Review Letters, 91(22), 227203.

[119] Wernsdorfer, W. (2007). Molecular magnets: A long-lasting phase. Nature Materials, 6(3), 174.

[120] Sieber, A., Foguet-Albiol, D., Waldmann, O., Ochsenbein, S. T., Carver, G., Mutka, H., et al. (2006). Pressure dependence of the exchange interaction in the dimeric single-molecule magnet $[Mn_4O_3Cl_4(O_2CEt)_3(py)_3]_2$ from inelastic neutron scattering. Physical Review B, 74(2), 024405.

[121] Wernsdorfer, W. (2008). Comment on: Quantum interference of tunnel trajectories between states of different spin length in a dimeric molecular nanomagnet. arXiv:0804.1246v3 [cond-mat.mes-hall].

[122] Ramsey, C. M., del Barco, E., Hill, S., Shah, S. J., Beedle, C. C., and Hendrickson, D. N. (2008). Reply to Wernsdorfer's post:" Correspondence on: Quantum interference of tunnel trajectories between states of different spin lenght in a dimeric molecular nanomagnet. arXiv:0806.1922v1 [cond-mat.mes-hall].

[123] Wernsdorfer, W., Bhaduri, S., Tiron, R., Hendrickson, D. N., and Christou, G. (2002). Spin-spin cross relaxation in single-molecule magnets. Physical Review Letters, 89(19), 197201.

[124] Kim, G. H. (2003). Tunneling in a single-molecule magnet via anisotropic exchange interactions. Physical Review B, 68(14), 144423.

[125] Bozat, Ö., and Gedik Z. (2008). Spin bath decoherence mediated by phonons. in press at Solid State Communications, doi:10.1016/j.ssc.2008.08.008.

[126] Abragam, A. (1961). The Principles of nuclear magnetism. Oxford University Press, London.

[127] Paganelli, S., de Pasquale, F., and Giampaolo, S. M. (2002). Decoherence slowing down in a symmetry-broken environment. Physical Review A, 66(5), 52317.

[128] Coffman, V., Kundu, J., and Wootters, W. K. (2000). Distributed entanglement. Physical Review A, 61(5), 52306.

[129] Koashi, M., Buek, V., and Imoto, N. (2000). Entangled webs: Tight bound for symmetric sharing of entanglement. Physical Review A, 62(5), 50302.

[130] Dawson, C. M., Hines, A. P., McKenzie, R. H., and Milburn, G. J. (2005). Entanglement sharing and decoherence in the spin-bath. Physical Review A, 71(5), 52321.

[131] Osborne, T. J., and Verstraete, F. (2006). General monogamy inequality for bipartite qubit entanglement. Physical Review Letters, 96(22), 220503.

[132] Ou, Y. C. (2007). Violation of monogamy inequality for higher-dimensional objects. Physical Review A, 75(3), 34305.

[133] Hiroshima, T., Adesso, G., and Illuminati, F. (2007). Monogamy inequality for distributed Gaussian entanglement. Physical Review Letters, 98(5), 050503.

[134] Duan, L. M., and Guo, G. C. (1997). Preserving coherence in quantum computation by pairing quantum bits. Physical Review Letters, 79(10), 1953.

[135] Zanardi, P., and Rasetti, M. (1997). Noiseless quantum codes. Physical Review Letters, 79(17), 3306.

[136] Ma, X. S., and Wang, A. M. (2007). The effect of stochastic dephasing on the entanglement and coherence of qutrits. Physica A, 386(1), 590.

[137] Jaeger, G., and Ann, K. (2007). Disentanglement and decoherence in a pair of qutrits under dephasing noise. Journal of Modern Optics, 54(16-17), 2327.

[138] Jóos, E. (2003). Decoherence through interaction with the environment. Decoherence and the appearance of a classical world in quantum theory (Edited by E. Joos, H. D. Zeh, C. Kiefer, D. Giulini, J. Kupsch and I.-O. Stamatescu, second edition), p. 41. Springer, Berlin.

[139] Sun, Z., Wang, X. G., Gao, Y. B., and Sun, C. P. (2008). Decoherence in time evolution of bound entanglement. The European Physical Journal D, 46(3), 521.

[140] Checinska, A., and Wodkiewicz, K. (2007). Separability of entangled qutrits in noisy channels. Physical Review A, 76(5), 052306.

[141] Bozat, Ö., and Gedik, Z. Dephasing in entangled qutrits. In preperation.

[142] Yu, T., and Eberly, J. H. (2003). Qubit disentanglement and decoherence via dephasing. Physical Review B, 68(16), 165322.